



JN-90
380 423
DATE OVERRIDE

TECHNICAL REPORT

R-149

AERODYNAMIC ANALYSIS OF TEKTITES AND THEIR PARENT BODIES

By E. W. Adams and R. M. Huffaker

George C. Marshall Space Flight Center
Huntsville, Alabama

**ADVANCE
COPY**

NATIONAL AERONAUTICS AND SPACE ADMINISTRATION

WASHINGTON

1962

[Faint, illegible text covering the majority of the page, possibly bleed-through from the reverse side.]

TECHNICAL REPORT R-149

AERODYNAMIC ANALYSIS OF TEKTITES AND THEIR PARENT BODIES

By E. W. Adams and R. M. Huffaker

ABSTRACT

Experiment and analysis indicate that the button-type australites were derived from glassy spheres which entered or re-entered the atmosphere as cold solid bodies; in case of average-size specimens, the entry direction was nearly horizontal and the entry speed between 6.5 and 11.2 km/sec. Terrestrial origin of such spheres is impossible because of extremely high deceleration rates at low altitudes. The limited extension of the strewn fields rules out extraterrestrial origin of clusters of such spheres because of stability considerations for clusters in space. However, tektites may have been released as liquid droplets from glassy parent bodies ablating in the atmosphere of the earth. The australites then have skipped together with the parent body in order to re-enter as cold spheres. Terrestrial origin of a parent body would require an extremely violent natural event. Ablation analysis shows that fusion of opaque siliceous stone into glass by aerodynamic heating is impossible.

INDEX HEADINGS

2
7
30
46
47



TECHNICAL REPORT R-149

AERODYNAMIC ANALYSIS OF TEKTITES AND THEIR PARENT BODIES

by E. W. Adams and R. M. Huffaker

SUMMARY

Experiment and analysis indicate that the button-type australites were derived from glassy spheres which entered or re-entered the atmosphere as cold solid bodies; in case of average-size specimens, the entry direction was nearly horizontal and the entry speed between 6.5 and 11.2 km/sec. Terrestrial origin of such spheres is impossible because of extremely high deceleration rates at low altitudes. The limited extension of the strewn fields rules out extraterrestrial origin of clusters of such spheres because of stability considerations for clusters in space. However, tektites may have been released as liquid droplets from glassy parent bodies ablating in the atmosphere of the earth. The australites then have skipped together with the parent body in order to re-enter as cold spheres. Terrestrial origin of a parent body would require an extremely violent natural event. Ablation analysis shows that fusion of opaque siliceous stone into glass by aerodynamic heating is impossible.

I. INTRODUCTION

Tektites are small glassy bodies which are found in well defined areas. The largest so-called strewn field covers most of Southeast Asia, and another strewn field covers most of Australia; smaller fields are located in Texas, Georgia, Ghana, Bohemia, and Moravia. All tektites have a family-like chemical composition and are unrelated to the geological formations in which they are found; therefore, they must have been hurled up somewhere by violent natural events and carried in flight into the strewn fields. Available evidence, e.g., radioactive dating, proposes, according to p. 118 of ref. 5, "that the different groups of tektites from the several zones of occurrence are separated in their time of arrival by considerable periods of time and that there must thus have been more than one shower of tektites during the earth's geological history." The material thrown up was either already glassy, due to meteor impact or volcanic action, or was fused into glass by aerodynamic heating in flight. In addition to such aerothermodynamic effects

during a hypothetical first flight phase in an atmosphere, all the australites and some javaites show a superficial second melting period resulting in a few peculiar types of surface sculpturings and well defined shapes, which can be explained by ablation during hypersonic flight in the earth's atmosphere, as will be shown in this paper.

It has not yet been possible to prove by chemical or physical analysis of natural tektites whether tektite-flight started at the earth's surface or at some extraterrestrial point of departure. The glassy uncrystallized substance includes 68% to 80% silica, 9% to 16% Al_2O_3 , etc. The complete absence of crystals and a slightly different chemical composition distinguish tektite glass from glassy ejecta, e.g., consisting of solidified ash from volcanic eruptions or from steam locomotives. According to Ref 2, very small quantities of nickel-iron spherules have been found among the minor constituents of some tektites. Since meteors are the only natural source of nickel-iron, meteor impact must then have caused the flight of tektites or of their parent bodies which released tektites in flight. Since Al^{26} with a half-life of 10^6 years is generated by prolonged exposure to cosmic radiation, its absence in 79 tektites taken from the Far East and Australia, according to Ref 3, yields the conclusions "(1) if tektites arrived as small unshielded bodies, their 'flight' or cosmic-ray exposure time was less than 10,000 years; (2) if they arrived in a large, well-shielded body, this 'prototektite' body must have had a radius ≥ 95 m".

The life expectation of a cluster of particles in arbitrary orbit in the solar system is very much longer than 10^4 years before an encounter with the earth, according to Ref 4. Stability reasoning (Ref 5), pertaining to solar gravitational forces, establishes a minimum density of 1 gram/ m^3 for such a cluster; i.e., "a swarm of this density some 10^8 cm in diameter would pile up tektites to a depth of 100 grams/ cm^2 over southern Australia, and this is not the case." Both these stability arguments and the Al^{26} test restrict the point of origin of tektite clusters to the earth moon system and thus demand a maximum entry speed of 11.2 km/sec, i.e., the escape speed of the earth.

These general statements are compatible with a large number of possible hypotheses about the origin of the tektites. Whereas the possibility of ablative shaping of tektites in flight has been discussed before in references 6, 7, 8, and 9, only the recent experimental and theoretical advances in the field of missile and space vehicle re-entry furnish the calculation methods needed to analyze tektite flight in the earth's atmosphere and thus to impose further restrictions on the variety of hypotheses. The available calculation methods for trajectory and ablation analysis are applicable if the object is a simple-

shaped body of revolution, consisting of a known material, and flying at zero angle of attack. With the exception of some uncertainty about material properties, these conditions are fulfilled for the button-type australites, whose final shape appears in the right column of fig. 1, as follows from Ref 10. The results to be discussed rest on the well-known trajectory equations for bodies of variable mass and on a calculation method for ablating glass or stone bodies. This method is described in Ref 11 and in unpublished reports by the same author. Comparison of ablation thicknesses calculated by use of this method to experimental ablation data for a glassy material shows less than 10% deviation.

The authors are indebted for very helpful discussions to Dr. John A. O'Keefe of the Goddard Space Flight Center (NASA) and Mr. Werner K. Dahm of the Marshall Space Flight Center (NASA). The assistance of Mr. Verk K. Eubanks for the IBM 7090 computer programming is gratefully acknowledged.

II. EVIDENCE FOR THE SHAPING OF THE BUTTON-TYPE AUSTRALITES BY AERODYNAMIC ABLATION IN DESCENDING FLIGHT

Chapman, in Ref 10, presents conclusive experimental proof that glass spheres, when placed in an electric-arc jet tunnel and exposed to heating rates of the order of those experienced in hypersonic flight, become strikingly similar to button-type australites, see fig. 1. This similarity comprises, first, a peculiar system of ring waves on the ablated front face, secondly, a coiled circumferential flange made of solidified melt, and finally, opposite the stagnation point and enclosed by the flange, a spherical remainder of the original surface shape. Fig. 2 shows a glass rod whose front face ablated in an electric-arc jet facility. The ring waves and the flange again are clearly visible in fig. 2. The existence of a systematic deformation of the striae which is confined to a very thin layer underneath the surface of both the natural and the artificial buttons shows, according to ref 10, that the ablation of the natural buttons was by aerodynamic heating of rigid glass and not by aerodynamic pressure acting on soft glass, since the latter would have distorted the striae pattern to a considerable depth below the surface. Chapman's work confirms beyond doubt that the anterior surface of the button-type australites was shaped by aerodynamic ablation acting on initially cold glassy spheres which, therefore, entered the atmosphere at high altitudes. Ablation and trajectory analyses are then applicable because the original spherical shape still exists at the posterior surfaces of the buttons.

The inspection of surface sculpturings on discovered australites reveals, according to Ref 1 and p. 19 of Ref 9, that they were derived from bodies of revolution and, in the majority of cases, from

spheres. Chapman points out on pp. 16 - 19 of Ref 10 that an oscillation about any axis other than the flight axis, whether initially present or induced by disturbances in flight, is rapidly damped by the continuously increasing magnitude of the surface pressure distribution in descending flight, whereas this damping effect would be absent in ascending flight. The decrease in curvature at the point where melting begins on a sphere causes a rearward departure of the aerodynamic center (of the pressure distribution) from the center of gravity. The corresponding unbalanced moment about the center of gravity tends to align the stagnation point of the body of revolution, the center of gravity, and the aerodynamic center, so that this will be the stable flight attitude.

A simple calculation yields an initial deceleration of 96,000 g for a solid glass sphere of 1.3 cm radius with an initial speed of 8 km/sec at sea level altitude. This, together with Chapman's above mentioned stability reasoning, rules out the departure of a cluster of tektites from the surface of the earth.

III. TRAJECTORY AND ABLATION ANALYSIS FOR THE FINAL DESCENT OF THE BUTTON-TYPE AUSTRALITES

By employing the steady-state approximation derived in Ref 12 for the ablation process, Chapman (Ref 13) was the first to analyze the descent of button-type australites under the assumption of small or moderate ablative mass losses so that the variable mass could be approximated in the trajectory calculations by the average of the masses at the beginning and at the end of the flight. Ref 14 presents a summary of a renewed study, to be discussed extensively in this section, of the final descent of button-type australites by employing combined non-stationary trajectory and ablation analysis to obtain results for the melting and evaporation history up to 100% ablation (see also Ref 15).

The geometric model employed for the calculations is a body of revolution which flies at zero angle of attack. If one-dimensional conduction of heat is assumed along the body axis $O-S_0$ in fig. 4, the flows of heat and mass may be determined on $O-S_0$ without reference to the neighbouring cross sections. The front face ablation of the glass spheres from which the button-type australites were derived and the formation of a flange can be approximated by a simplified model that is hemispheric at the entry altitude $H = 150$ km above sea level. In order to check the dependence of the results on the geometric model employed, an initially spherical model was also investigated whose front half is supposed to ablate as shown in fig. 4. A comparison of results for the two models indicates very little difference (table 1). The calculated results prove that the flow of air is laminar on the entire surface of the assumed hemispheric model during the ablation period. Other studies (e.g., Ref 11)

show that the total ablation decreases under this condition as the distance from the stagnation point increases. The ablation process which is calculated only along $O-S_0$, is supposed to convert the hemispheric shape $A-S_0-B-O-A$ in fig. 4 into the section $A-S(t)-B-O-A$ of a sphere completely defined by the thickness $R^*(t)$ of the model. The weights of the glass spheres from which the button-type australites were derived by ablation vary in the limits 1.4 - 28 grams, according to fig. 3. This yields the limiting initial radii $R(0) = 0.65$ cm and $R(0) = 1.78$ cm of the hemispheric model. Results have been calculated for the radii $R(0) = 0.65$ cm and $R(0) = 1.30$ cm, which correspond to initial weights 1.38 and 11.04 grams, respectively. A constant drag coefficient of $c_D = 2.5$ was assumed for the trajectory calculations in the free-molecular region of the air; c_D was calculated as a function of $R^*(t)/R(0)$ and the flight Mach number, $M(t)$, in the continuum flow region of the air. The trajectory and ablation analysis was carried out on an IBM 7090 computer by use of time steps between 10^{-3} and 10^{-1} sec. The following material properties of the supposedly opaque material were employed in the calculations: thermal conductivity $k = 5 \times 10^{-4}$ kcal/m °K sec according to p. 162 of Ref 1; specific heat $c_p = 0.21$ kcal/kg °K according to Ref 16; surface emissivity constant $\epsilon = 0.4$ (estimated); and viscosity function $\mu(T) = 0.0102 \exp [(44,891/T \text{ °K}) - 14.541]$ kg sec/m² according to Ref 17. Since measurements of the vapor pressure $p_v(T)$ of tektite material have not yet been published, the actually employed function, namely, $p_{v1}(T) = 13.595 \exp [30.01 - (57,250/T \text{ °K})]$ kg/m², was obtained from the vapor pressure of fused silica, $p_{v2}(T) = 15,498 \exp [18.41 - (58,176/T \text{ °K})]$ kg/m², Ref 18, by lowering the boiling point at one atmosphere from 3070°K to 2500°K to account for the volatile component in tektites, whose silica content is only 68% - 80%.

For the initially hemispheric model of button-type australites shown in fig. 4 with the material properties listed in the preceding paragraph, figures 5 through 15 present curves of constant performance parameters as functions of entry speed V_i km/sec and entry angle θ_i at entry altitude $H = 150$ km above sea level. The material properties were changed in a few typical cases to take the following values: first, $k = 4 \times 10^{-4}$ kcal/m °K sec and $c_p = 0.29$ kcal/kg °K and second, $\epsilon = 0.05$. The resulting changes in the relative mass loss, $[1 - m(t_f)/m(0)]$, are smaller than 6% as compared to the results presented in fig. 5. The comparison of the solid lines in figures 5 and 6 shows, however, that the uncertainty about the vapor pressure of tektite material has considerable effect on the results.

The curves for $R(0) = 1.3$ cm (initial weight of 11.04 grams) in figures 5 and 6 are typical for the discovered button-type australites since the spheres defined by the radii of the posterior surfaces of natural buttons have an average weight of 11 grams, according to p. 79 of Ref 1. The range of possible entry conditions can then be limited

as follows in figures 5 and 6: (1) by the overshoot line since the final descent is considered, (2) according to fig. 3, by the ablation range of 70% - 90% for natural buttons with an initial weight of 11 grams, and (3) by the earth's escape speed, 11.2 km/sec. The last condition is valid for both a cluster of tektites entering the earth's atmosphere for the first time, according to evidence in section I pertaining to the extraterrestrial origin of such a cluster, and also for re-entering solidified droplets which were released from an ablating parent body in a manner to be described in section IV. The possible entry conditions are then $7 \leq V_i \leq 11.2$ km/sec and $0 \leq \theta_i \leq 6^\circ$ in case of the function $p_{V1}(T)$ and $6.5 \leq V_i \leq 11.2$ km/sec and $0 \leq \theta_i \leq 29^\circ$ in case of the function $p_{V2}(T)$.

Table 2, which follows from evaluating figures 5 through 15, explains the dependence of the results on the relevant parameters V_i , θ_i , $m(0)$, and $p_V(T)$. This dependence is predominantly determined by the aerodynamic heating pulse and by the shielding mass transfer effect. A smaller percentage of the kinetic energy converted into heat reaches the surface as the heat pulse is shifted to lower altitudes, where a higher portion of the generated heat remains in the denser air. The case is clearest for the change of θ_i since this causes no change in the kinetic energy and only a relatively small increase in the mass transfer effect according to table 2.

Any rise of the enthalpy difference ($h_e - h_s$) across the air boundary layer causes an increase of the surface temperature T_s and, correspondingly of the flow rate and evaporation rate of melt and of the emission of radiation from the surface. The vaporization process absorbs heat; also, the heat transfer coefficient, h , decreases due to the diffusion of vapor across the air boundary layer. The aerodynamic heat transfer rate at the wall, $q_{aero}(t) = h(h_e - h_s)$ kcal/m² sec, therefore, increases at a smaller rate than the enthalpy difference ($h_e - h_s$). Since there is only convective heating and negligible gas radiation for the small bodies under discussion, the surface temperature may tend toward the boiling point but it cannot reach this point. If the intensity of the heat pulse increases at a constant altitude, as in case of a rise of V_i , small increases of the surface temperature are sufficient to raise both the evaporation rate and the shielding mass transfer effect at such a steep rate as to cope with any increase of ($h_e - h_s$). If the heat pulse is shifted to lower altitudes, the evaporation rate decreases unless the surface temperature considerably rises, as table 2 shows for an increase θ_i . The large shielding mass transfer effect explains why bodies as small as tektites may enter at velocities of 20 km/sec, where the aerodynamic heat transfer reaches the order of 80,000 kcal/m² sec in case of vertical entry, and still arrive at the earth's surface with only moderate mass loss, see figures 5 and 14.

If the higher vapor pressure function $p_{V1}(T)$ is replaced by the lower function $p_{V2}(T)$, the necessary shielding mass transfer effect requires

considerably higher surface temperatures and, therefore, is accompanied by higher melt flow rates (table 2). The comparison of the solid lines in figures 5 and 6 indicates a strong increase of the relative mass loss $[1 - m(t_f)/m(0)]$ when $p_{V2}(T)$ is substituted for $p_{V1}(T)$.

As an example for the 100 calculated solutions, figures 16 through 21 present one special solution which is defined by the entry speed $V_i = 9$ km/sec, the entry angle $\theta_i = 7^\circ$ relative to the earth's horizon, the entry altitude $H = 150$ km above sea level, the vapor pressure function $p_{V1}(T)$, and the initial radius $R(0) = 1.3$ cm of the hemispheric model. The flight terminates at sea level altitude, $H = 0$ km, with the impact speed $V_f = 17$ m/sec and the nearly vertical impact angle $\theta_f = 89.99^\circ$. The last calculated temperature profile along the axis of symmetry is nearly uniform with $T = 780^\circ\text{K}$ at the altitude $H = 11.54$ km according to fig. 20; i.e., the body already has become rigid some time before impacting. It is seen that the aerodynamic heat pulse, $\bar{q}_{aero}(t)$, takes place at a slightly higher altitude than the deceleration pulse, $a(t)$. The maximum deceleration has a value of 26 g. The ablation at the stagnation point, 43% of which is due to evaporation, starts in the free-molecular region of the air at 90 km altitude and ends in the hypersonic continuum flow region at flight Mach numbers > 4 . The surface temperature closely follows the change of the aerodynamic heat transfer pulse $\bar{q}_{aero}(t)$.

For the initially hemispheric button model, whose performance as a function of time has been discussed in the preceding paragraph, fig. 20 presents temperature profiles $T = T(z,t)$ °K along the body's z-axis as following from one-dimensional heat conduction analysis. The shaded portions adjacent to the instantaneous locations of the surface indicate the thickness of the melt flow. The deepest penetration of the molten layer is reached at time $t = 100$ sec when resolidification has just started. The corresponding calculated striae deformation due to previous melt flow in the solidified layer is shown in fig. 21a for the vicinity of the stagnation point. The straight line in fig. 21b shows the striae distortion as a function of the distance x from the stagnation point and the lines in fig. 21c feature the striae profiles underneath the surface for two distances x from the stagnation point. Fig. 22 shows the corresponding results for the striae deformation in case of an initially hemispheric model which enters with a speed of $V_i = 6$ km/sec and the angle $\theta_i = 2^\circ$ and which suffers only 29% ablation in flight.

The following additional general conclusions can be drawn from the calculated cases: The impact at sea level altitude takes place in the range $88^\circ \leq \theta_f \leq 90^\circ$, i.e., in a nearly vertical direction. The impact speed is limited by $V_f \leq 28$ m/sec. The temperature level on the line $0-S(t)$ defined in fig. 4 is below 600°K at impact time, so that plastic deformations due to the impact are impossible.

IV. THE PARENT BODY HYPOTHESIS FOR TEKTITE ORIGIN

According to Sections II and III, a combination of experiment, observation, and analysis shows that the button-type australites were cold glassy spheres which entered the earth's atmosphere at high altitude. This entry took place in a nearly horizontal direction and with velocities in excess of 6.5 km/sec in case of average size buttons. Trajectory analysis in Section II indicates that bodies as small as tektites hurled up from sea level cannot traverse the atmosphere to re-enter under these conditions. This proves that ejecta hurled up by impact on the surface of the earth cannot form a tektite cluster. Ejecta hurled up by impact on any extraterrestrial body in the solar system, generally stay in space for very long periods of time and, if approaching the earth, do not arrive in a dense and short-lasting shower, as is demanded by the existence of a few and relatively small tektite strewn fields (see Ref 5). These arguments show that tektite showers could not have originated as clusters of individual tektites by impact on the earth or any other celestial body.

The existence of limited tektite strewn fields could be explained if tektites were released as liquid fragments from the ablating surface of a hypothetical parent body in hypersonic flight in the earth's atmosphere. Hardcastle and Hanus stipulated in References 7 and 8 that the surface of a stony meteor melted during hypersonic flight in the atmosphere and sprayed liquid droplets, which gave rise to the characteristic forms of tektites while cooling off. In general, however, aerodynamic heating rates in high speed flight are so great that the molten layer on the surface of a stony meteor is extremely thin, because of the low thermal diffusivity of stone and the almost immediate evaporation of the melt. O'Keefe pointed out in Ref 19 that the evaporation rate of the melt might become sufficiently small if a grazing orbit with small instantaneous heat transfer rates is considered, like the one of the Cyrillid shower. According to trajectory calculations published in Ref 20, only those liquid droplets which are released during the final stages of such a shallow orbit in the earth's atmosphere exit together with the parent meteor, so that re-entry is possible in the way it has been described for the button-type australites in Section III.

By applying a calculation method presented in Ref 11 and in unpublished reports, the authors have studied the ablation of stony and glassy objects in high speed flight in the atmosphere of the earth. The physical aspects of the underlying ablation processes are summarized in the following. Since the thickness of the hot gas layer between the shock front and the surface increases together with the cross section of a body in supersonic flight, the obviously large parent bodies are predominantly heated by radiation emitted from the hot gas layer, whereas bodies as small as tektites essentially experience convective heating only. Detailed calculations show that the extremely high radiation rates of as much as

$10^4 - 10^6$ kcal/m² sec, which are incident at the surface of a large parent body in hypersonic flight, cause the surface to boil. If the material is opaque to thermal radiation, the heated layer beneath the rapidly receding surface has a thickness of considerably less than 1 mm; obviously, only negligible amounts of liquid material could then be released from the parent body. The calculations show, however, that a layer of several cm thickness reaches temperatures of 3000 to 5000°K if the material is sufficiently transparent to thermal radiation. In one special case, the thickness of the radiatively heated layer turned out to be 5 cm for the absorption coefficient $\alpha = 100$ (1/m) of clear window glass and 0.6 cm for $\alpha = 1000$ (1/m). Vapor nuclei are then formed at non-homogeneous spots in the glassy melt. Unless strong temperature gradients normal to the surface exist in the melt, there is no force present which drives the bubbles towards the surface. The outer portions of the radiatively heated layer, therefore, consist of a spongy glass melt which offers little resistance to being removed from the parent body by the air forces acting in hypersonic flight. Since this mechanism rests on the existence of sufficiently high temperatures in the spongy layer, the detached fragments possess low viscosity and break up readily in the air stream. The outlined process implies that the parent body consists of a glassy material whose chemical composition is similar to the one of tektites. This glassy substance cannot be generated by fusion of siliceous stone due to aerodynamic heating, because the transparency of stone is too low to allow a radiatively heated layer of sufficient thickness. (See the numbers quoted above.)

If tektites became detached from an ablating glassy parent body which was hurled up by some violent natural event from the earth's surface, the parent body must have been sufficiently rigid at the time of departure in order to avoid immediate disintegration. The initial speed must have been sufficiently high and the initial trajectory angle sufficiently shallow if an area of the size of Australia is to be covered by fragments of this body or a cluster of large bodies hurled up by the same event. Figure 23 presents exit speed and exit angle at 150 km altitude above sea level for non-ablating spheres of specific weight 2.4 grams/cm³, which depart from sea level altitude at an angle of five degrees relative to the horizon. The ascending spheres must exit from the atmosphere with at least the previously derived minimum entry speed, 6.5 km/sec, of button-type australites if average-size buttons are released from these spheres. According to fig. 23, the exit speed of 8 km/sec requires an initial speed of 24 km/sec for a body of 46,000 tons and 12 km/sec for a body of 1.05×10^6 tons. Solid fragments hurled up from terrestrial volcanic eruptions or impact craters are known to be considerably smaller than 10^4 tons and to have traveled only short distances. Since initial speeds at sea level altitude in excess of 12 km/sec cause very high ablative mass loss rates, the parent body rapidly shrinks. As compared to the results in fig. 1, which pertains to non-ablating parent bodies, considerably larger initial weights and velocities are necessary to obtain an exit speed - 6.5 km/sec

at 150 km altitude. The extremely large initial acceleration rates, going together with the initial flight speeds under discussion, subject the impact-ejecta to surface and internal stresses which causes immediate disintegration, regardless of whether the material is in the liquid or in the solid state. The presented arguments show that individual tektites and their hypothetical parent bodies could not have been hurled up from the surface of any planet covered by a dense atmosphere, unless one stipulates an extremely violent natural event of such magnitude as to cause the atmosphere to be essentially "blown out." Urey has suggested in Ref 5 a comet-earth collision as being a possible origin of the tektites.

Characteristic features of the Indomalayan and Australian tektite strewn fields can be explained if a parent body of extraterrestrial origin in hypersonic skipping flight in the atmosphere is considered. The vapor bubbles in spongy droplets which skip together with the parent body expand continuously in ascending flight because of the decrease of the external pressure. The bubbles, correspondingly, tend to burst under this condition, and surface tension converts sufficiently small droplets into relatively compact glassy spheres. Since the majority of the australites were derived from glassy spheres, according to references 1 and 10 the described ablation mechanism implies that the parent body carried out a skipping flight pass in the earth's atmosphere and released the australites during the ascending flight phase so that they could exit together with the parent body.

The droplets which became detached from the parent body and did not exit from the atmosphere remained in the liquid state until they slowed sufficiently in the denser layers of the atmosphere. Because of the increasing pressure forces exerted by the air stream in descending flight, surface tension did not shape these droplets which, at the same time, remained spongy. Due to a lack of well-defined shape, the non-skipping liquid droplets in general did not possess stable flight attitude so that traces of previous melt flow should appear only in exceptional cases on the solidified surfaces. Since the relatively frothy indochinites and philippinites usually do not possess any well-defined shape and hardly any markings of melt flow, it may be concluded that these groups of tektites from the Indomalayan strewn field became detached from the parent body and descended immediately without a preceding skipping phase.

Liquid droplets released during the ascending flight phase of a skipping parent body may exit from the atmosphere with any vertical velocity component between zero and the one of the parent body. The droplets take spherical shape only if they fly outside of the atmosphere for a sufficient period of time. The necessary minimum flight time outside of the atmosphere decreases together with the size of the droplets, and thus also the necessary vertical component of exit speed.

The mass loss of the smallest discovered button-type australites (1.4 grams initial weight according to fig. 3) correspondingly varies in the limits 20% - 80%. Figure 5 indicates that a mass loss of 20% in case of a button of 1.38 grams initial weight requires an entry speed of less than 5 - 7 km/sec. This entry speed is considerably smaller than the minimum velocity at which an extraterrestrial object arrives at the earth. In addition to the previously presented argument pertaining to the size of the strewn fields, the existence of small button-type australites with mass losses of $\geq 20\%$ confirms the parent body hypothesis and rules out, e.g., direct departure of a cluster of spheres from the moon. Droplets which are too large to be shaped by surface tension or which do not stay outside of the atmosphere long enough, cannot take spherical shape and may then account for the australites which were derived from general bodies of revolution, e.g., the canoe-shaped forms described in ref. 5.

The droplets were closely spaced in the parent body's wake at the time of their release. The pressure fields surrounding the individual droplets, therefore, induced velocity components normal to the flight direction of the parent body. This, together with turbulence in the wake of the parent body, as pointed out by O'Keefe in ref. 16, explains why droplets released from a parent body can cover strewn corridors of some lateral extension along the projection of the parent body's trajectory. The width of the Indomalayan strewn field possibly cannot be explained by these two effects. It may be necessary, therefore, to assume that the parent body broke up during a first skipping pass through the atmosphere.

Since the outlined ablation mechanism removes material from the surface of the parent body, the previously mentioned absence of Al^{26} in discovered tektites (ref.22) implies a flight time in space of less than 10^4 years. The Al^{26} test thus rules out any origin of parent body flight more distant than the moon.

CONCLUSIONS

Experiment and analysis indicate that button-type australites were derived by aerodynamic heating from initially cold glassy spheres which, in case of average-size specimens, entered the atmosphere in a nearly horizontal direction between 6.5 and 11.2 km/sec; the lower limit, 6.5 km/sec, is demanded by the observed mass loss, 70% - 90%, of average-size buttons. Trajectory analysis shows that terrestrial origin of the spheres is impossible. Since the smallest discovered buttons, according to ablation analysis, must have entered at less than 7 km/sec, extraterrestrial origin of tektite clusters is impossible. The existence of limited tektite strewn fields can be explained if tektites were released as liquid droplets from the ablating surface of a hypothetical parent body in skipping flight through the earth's atmosphere. Ablation analysis

shows that this parent body must consist of a glassy substance, which cannot be generated by fusion of siliceous stone due to aerodynamic heating. Terrestrial origin of such a parent body, even when the material is not in the liquid but in the solid state, would require a violent event of such magnitude as to be very unlikely to have ever occurred. While aerodynamic analysis thus shows the extraterrestrial origin of parent bodies, the lack of cosmic-ray induced Al^{26} in discovered tektites seems to rule out flight more distant than the moon.

TABLE 1

Comparison of Results for Initially Spherical
and Initially Hemispherical Models

	Trajectory Parameters				$\frac{m(t_f)}{m(0)}$	$T_{s_{max}}$	$\frac{\int_0^{t_f} v_s dt}{\int_0^{\infty} v dt}$
	V_i	θ_i	$R(0)$	$W(0)$			
	km/sec	deg	cm	gms		$^{\circ}K$	
Initially Spherical Model	8	10	1.30	22.08	.640	2206	.427
	8	90	1.30	22.08	.802	2385	.444
Initially Hemispherical Model	8	10	1.30	11.04	.601	2143	.451
	8	90	1.30	11.04	.767	2300	.467
Initially Spherical Model	8	10	1.032	11.04	.598	2159	.428
	8	90	1.032	11.04	.760	2348	.445

TABLE 2

Interpretation of Figures 5 through 15

Parameter	Symbol and Physical Unit	Figure Number	Increase Entry Flight Speed V_i	Increase of entry Flight Angle θ_i in the range $0 < \theta_i < 30^\circ$	Increase of Entry Mass $m(0)$	Increase of vapor pressure Level
Kinetic Energy Converted into Heat	$\frac{m(0)V_i^2}{2}$ [mkg]		Increase proportional to V_i^2	No Change	Increase Proportional to $m(0)$	No Change
Relative Mass Loss	$1 - \frac{m(tf)}{m(0)}$	5&6	Moderate Increase	Strong Decrease	Moderate Decrease	Strong Decrease
Horizontal Distance Covered in Flight	D [km]	7	Nearly constant	Very Strong Decrease	Small Increase	Nearly Constant
Ratio of Aerodynamic Heat Transfer to Kinetic Energy Converted into Heat	$\int_0^{t_f} \bar{q}_{aero}(t) dt \left[\frac{kcal}{m^2} \right]$ $\frac{m(0)V_i^2}{2A} \left[\frac{mkg}{m^2} \right] \left[\frac{kcal}{427 mkg} \right]$	8	Small Increase	Small Decrease		Very Small Increase
Altitude where Maximum of Aerodynamic Heat Pulse Occurs	H^* [km]	9	Small Increase	Moderate Decrease	Small Decrease	No Change
Duration of Aerodynamic Heating Pulse	Δt [sec]	10		Strong Decrease	Moderate Increase	No Change
Maximum Surface Temperature	$T_{s,max}$ [$^\circ K$]	11	Small Increase	Moderate Increase	Moderate Increase	Strong Decrease
Maximum Aerodynamic Heating Rate	$\bar{q}_{aero, max}$ $\left[\frac{kcal}{m^2 sec} \right]$	12	Strong Increase	Strong Increase	Moderate Increase	Very Small Increase

TABLE 2 (Cont'd)

Interpretation of Figures 5 through 15

Parameter	Symbol and Physical Unit	Figure Number	Increase of Entry Flight Speed V_i	Increase of Entry Flight Angle θ_i in the range $0 < \theta_i < 30^\circ$	Increase of Entry Mass $m(0)$	Increase of Vapor Pressure Level
Ratio of Heat Radiated from Surface to Aerodynamic Heating	$\frac{\int_0^{t_f} \bar{q}_{rad}(t) dt \left[\frac{\text{kcal}}{\text{m}^2} \right]}{\int_0^{t_f} \bar{q}_{aero}(t) dt \left[\frac{\text{kcal}}{\text{m}^2} \right]}$	13	Moderate Decrease	Moderate Decrease	Nearly Constant	Strong Decrease
Ratio of Heat Blocked by Mass Transfer Effect To Aerodynamic Heating	$\frac{\int_0^{t_f} \bar{q}_{bl}(t) dt \left[\frac{\text{kcal}}{\text{m}^2} \right]}{\int_0^{t_f} \bar{q}_{aero}(t) dt \left[\frac{\text{kcal}}{\text{m}^2} \right]}$	14	Moderate Increase	Small Increase	Very Small Increase	Strong Increase
Ratio of Evaporation to Total Ablation	$\frac{\int_0^{t_f} v_s(t) dt [\text{mm}]}{\int_0^{t_f} v_{\infty}(t) dt [\text{mm}]}$	15	Moderate Increase	Small Increase		Strong Increase

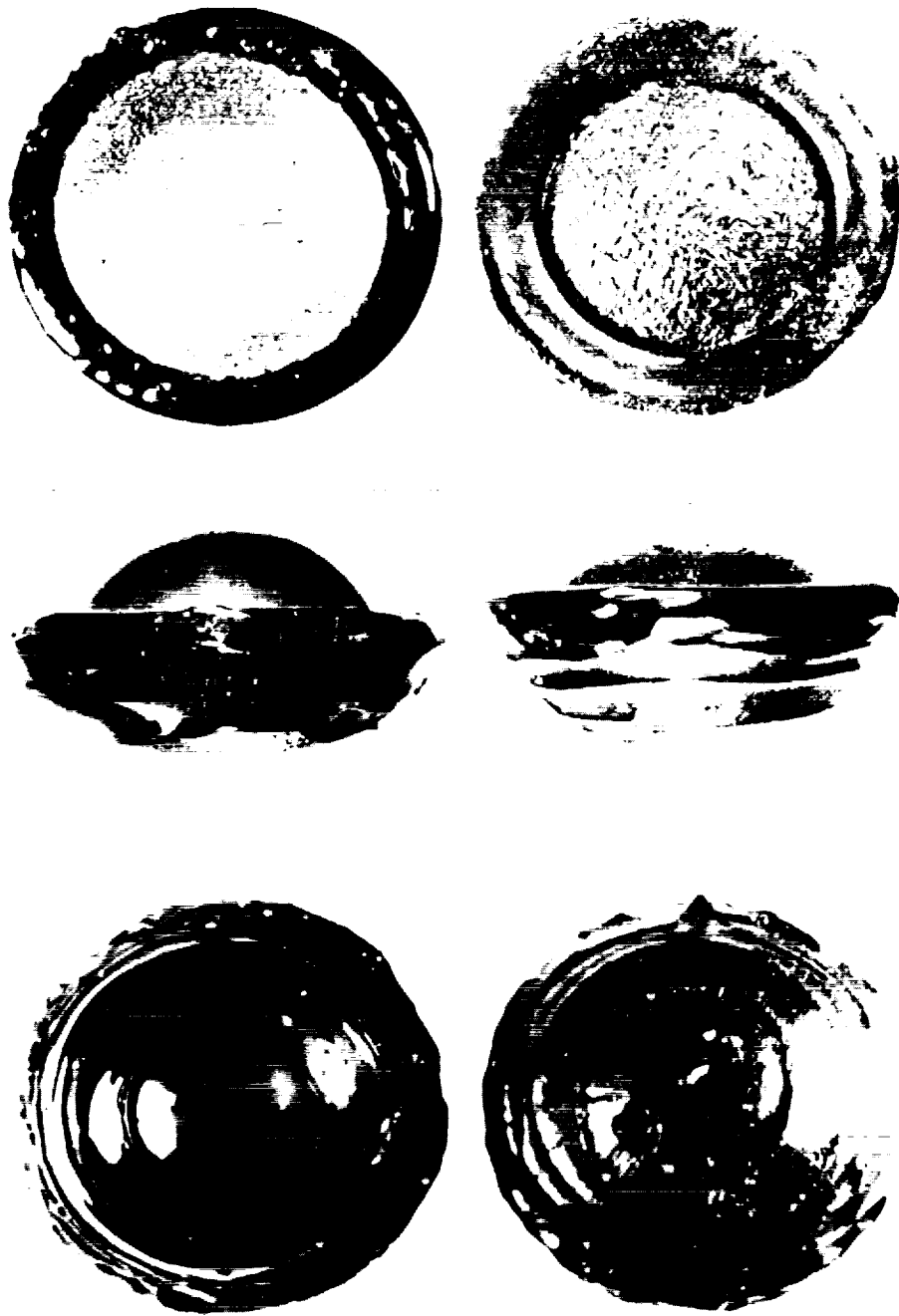
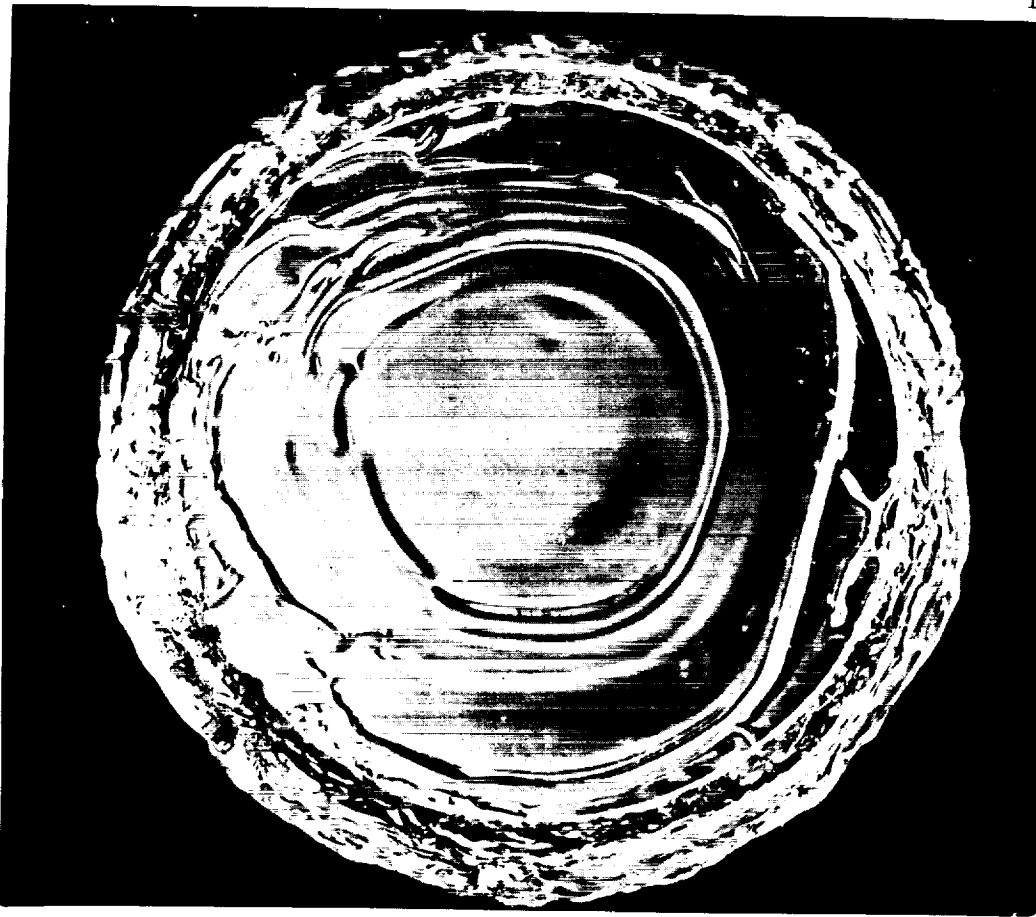


Fig. 1 COMPARISON OF NATURAL AND ARTIFICIAL BUTTON-TYPE AUSTRALITES

At right, three natural buttons on exhibition in the British museum; at left, three artificial button models ablated by aerodynamic heating. This photograph, which appears as fig. 9 in ref. 9 was made available through the courtesy of Dr. Dean R. Chapman of the Ames Research Center.



This photograph was made available through the courtesy of Dr. J. A. O'Keefe, Goddard Space Flight Center.

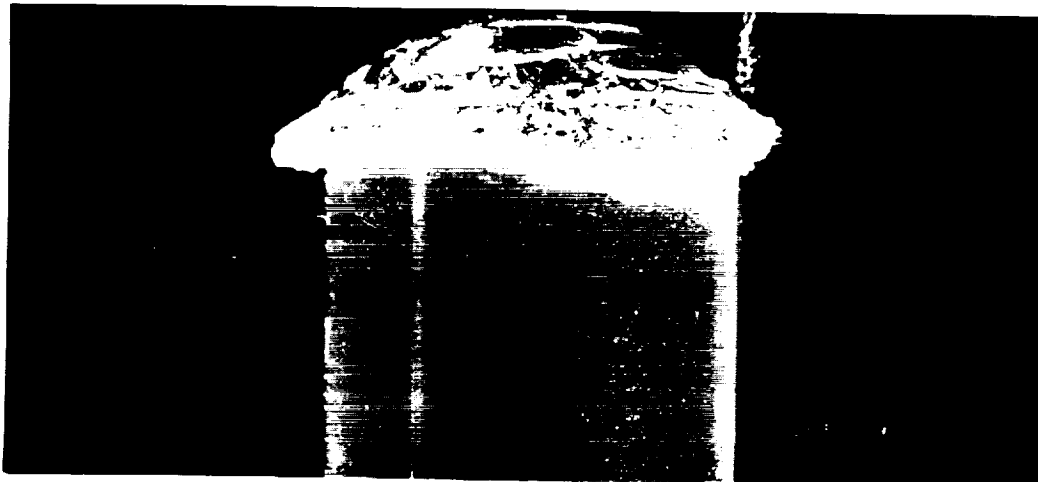


FIG. 2. GLASS ROD ABLATED IN AN ARC-JET FACILITY

This graph is taken from p. 79 of Ref. 5.

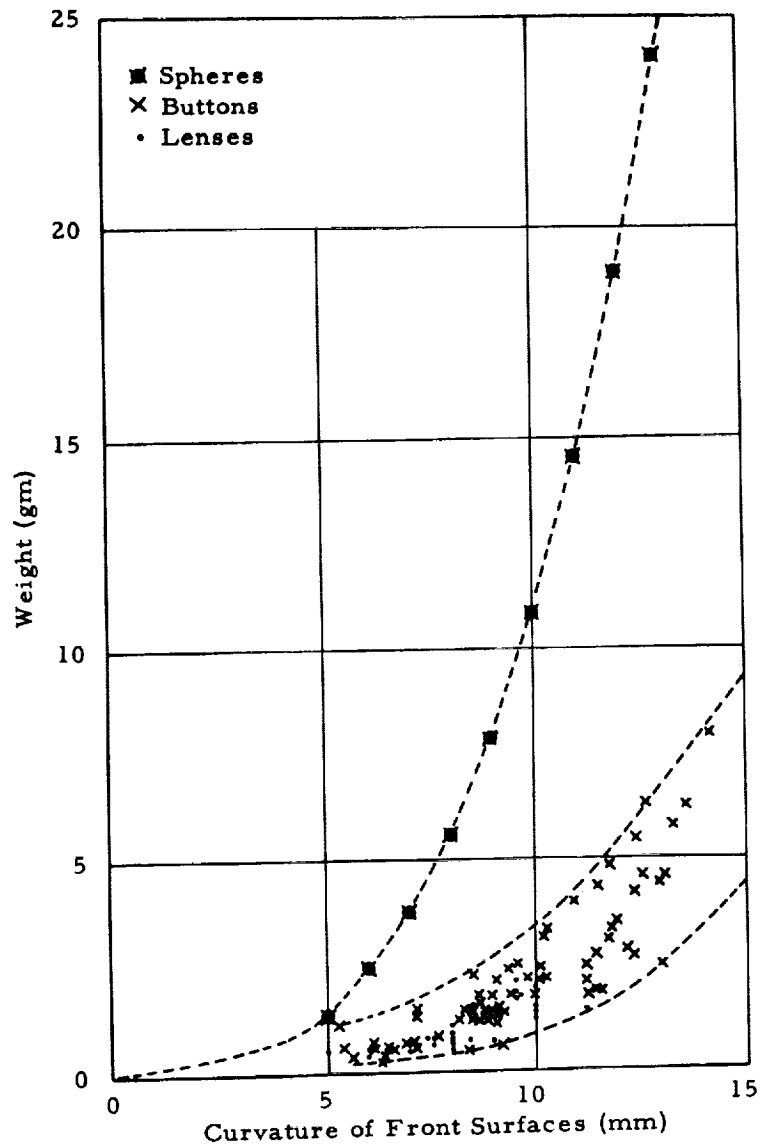


FIG. 3. WEIGHT VERSUS CURVATURE OF FRONT SURFACE OF BUTTON- AND LENS-TYPE AUSTRALITES

The ablation process is investigated along the axis S_0-O . S_0 = stagnation point before ablation begins; $S(t)$ = stagnation point during and after the end of the ablation period. Ablation is assumed to convert the hemispherical shape $A-S_0-B-O-A$ into the section $A-S(t)-B-O-A$ of a sphere.

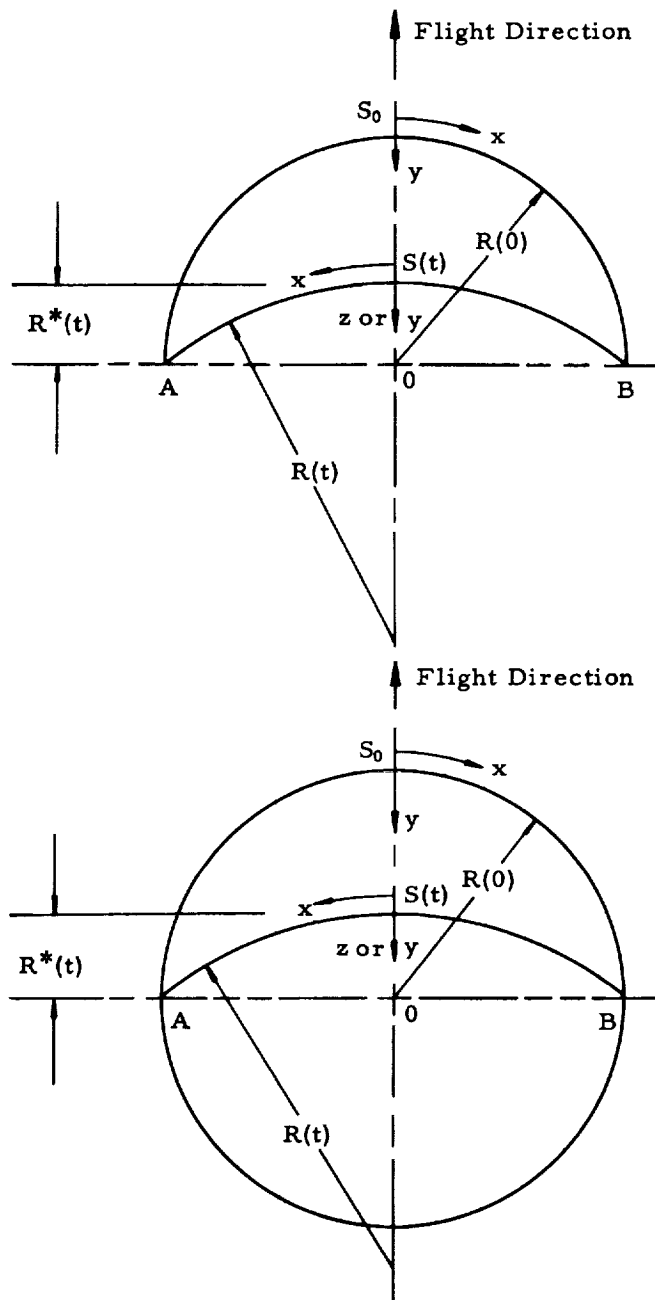


FIG. 4. GEOMETRIES OF INITIALLY HEMISPHERICAL AND SPHERICAL MODELS OF BUTTON-TYPE AUSTRALITES

20 Data pertains to vapor pressure function $p_{v1}(T)$ and initially hemispheric model with mass $m(0)$:
 Radius $R(0) = 1.30$ cm, i. e. $W(0) = 11.04$ grams (———)
 Radius $R(0) = 0.65$ cm, i. e. $W(0) = 1.38$ grams (----)
 $m(t_f)$ = final mass at impact time

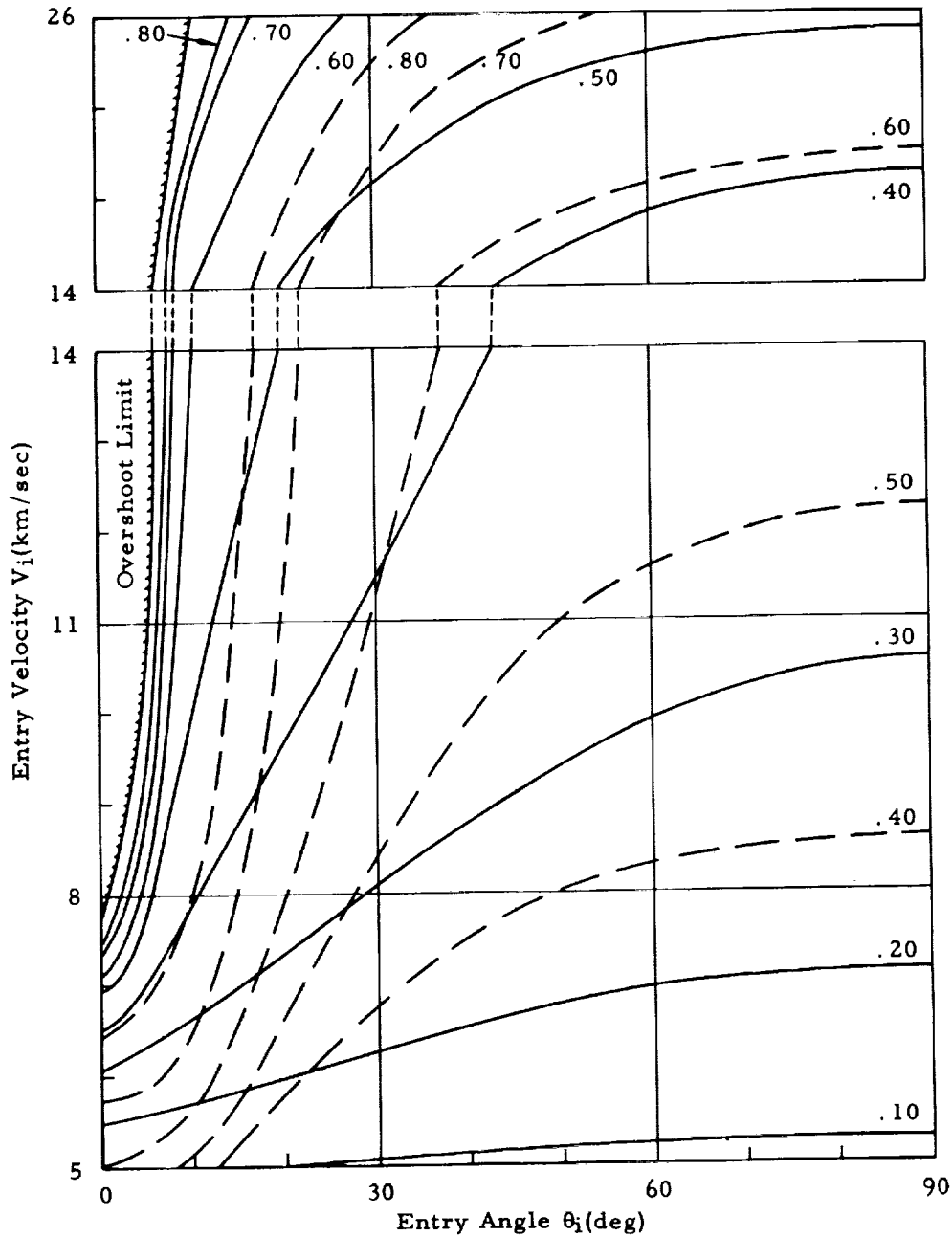


FIG. 5. RELATIVE MASS LOSS, $1 - m(t_f)/m(0)$

Data pertains to initially hemispheric model with mass $m(0)$, radius $R(0) = 1.30$ cm,
i.e. $W(0) = 11.04$ grams:

Vapor pressure function $p_{V1}(T)$ (—)

Vapor pressure function $p_{V2}(T)$ (-·-·-)

$m(t_f)$ = final mass at impact time

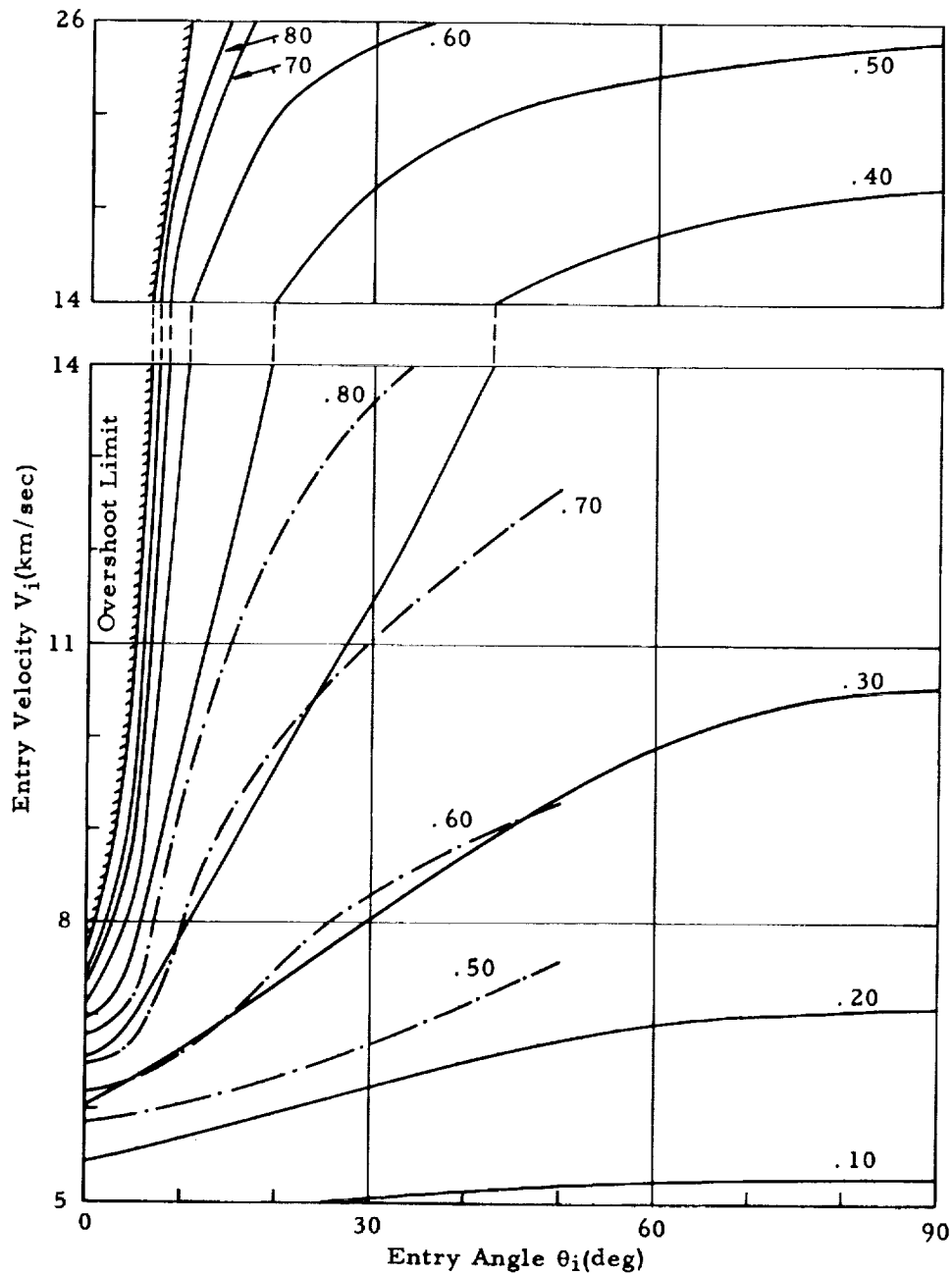


FIG. 6. RELATIVE MASS LOSS, $1 - m(t_f)/m(0)$

Data pertains to vapor pressure function $p_{v1}(T)$ and initially hemispheric model with:

Radius $R(0) = 1.30$ cm, i. e. $W(0) = 11.04$ grams (———)

Radius $R(0) = 0.65$ cm, i. e. $W(0) = 1.38$ grams (----)

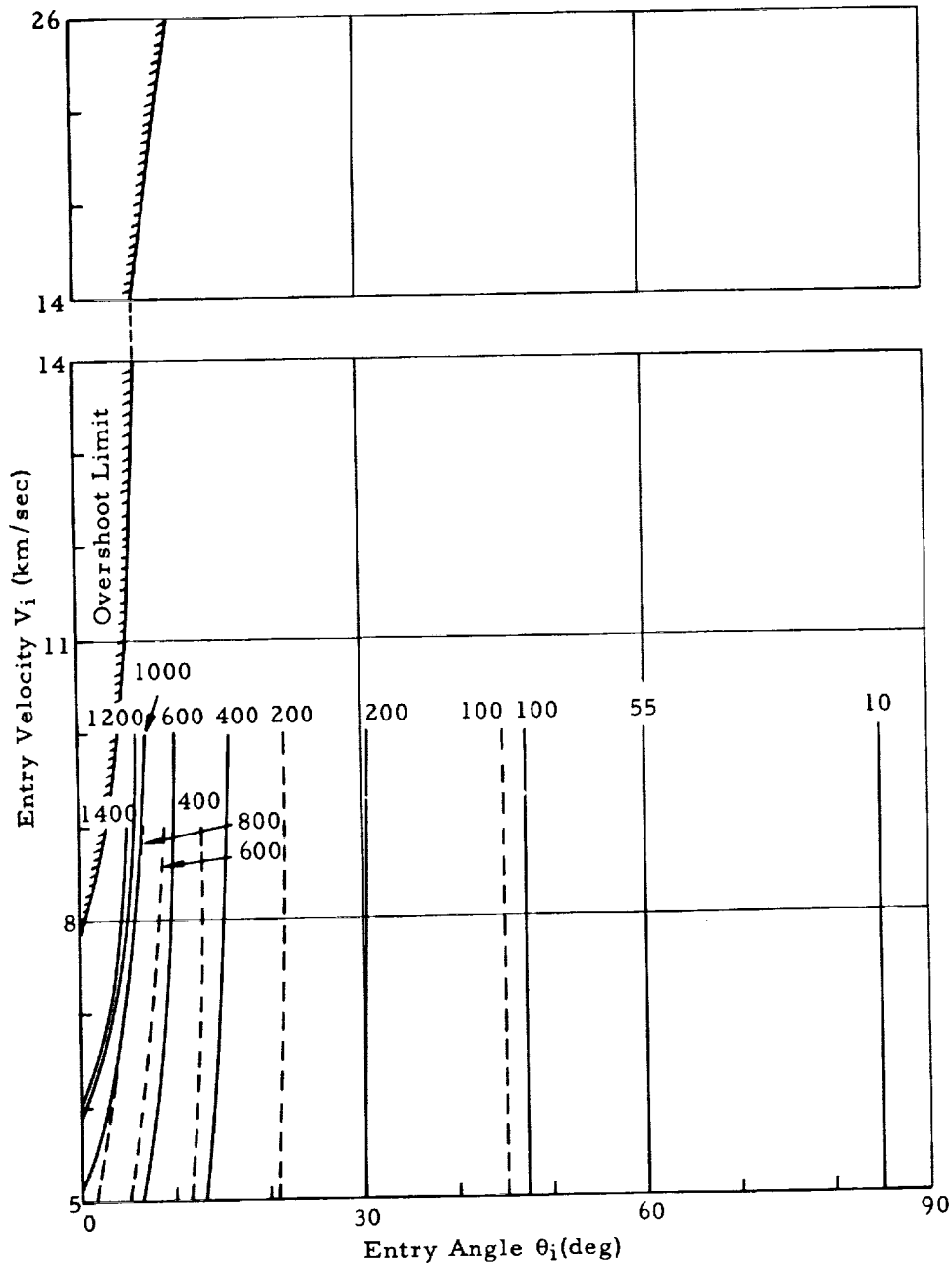


FIG. 7. HORIZONTAL DISTANCE $D(t)$ (KM)COVERED IN FLIGHT

Data pertains to initially hemispheric model with radius $R(0) = 1.30$ cm, 23
 i. e. $W(0) = 11.04$ grams, and vapor pressure function $p_{v1}(T)$.

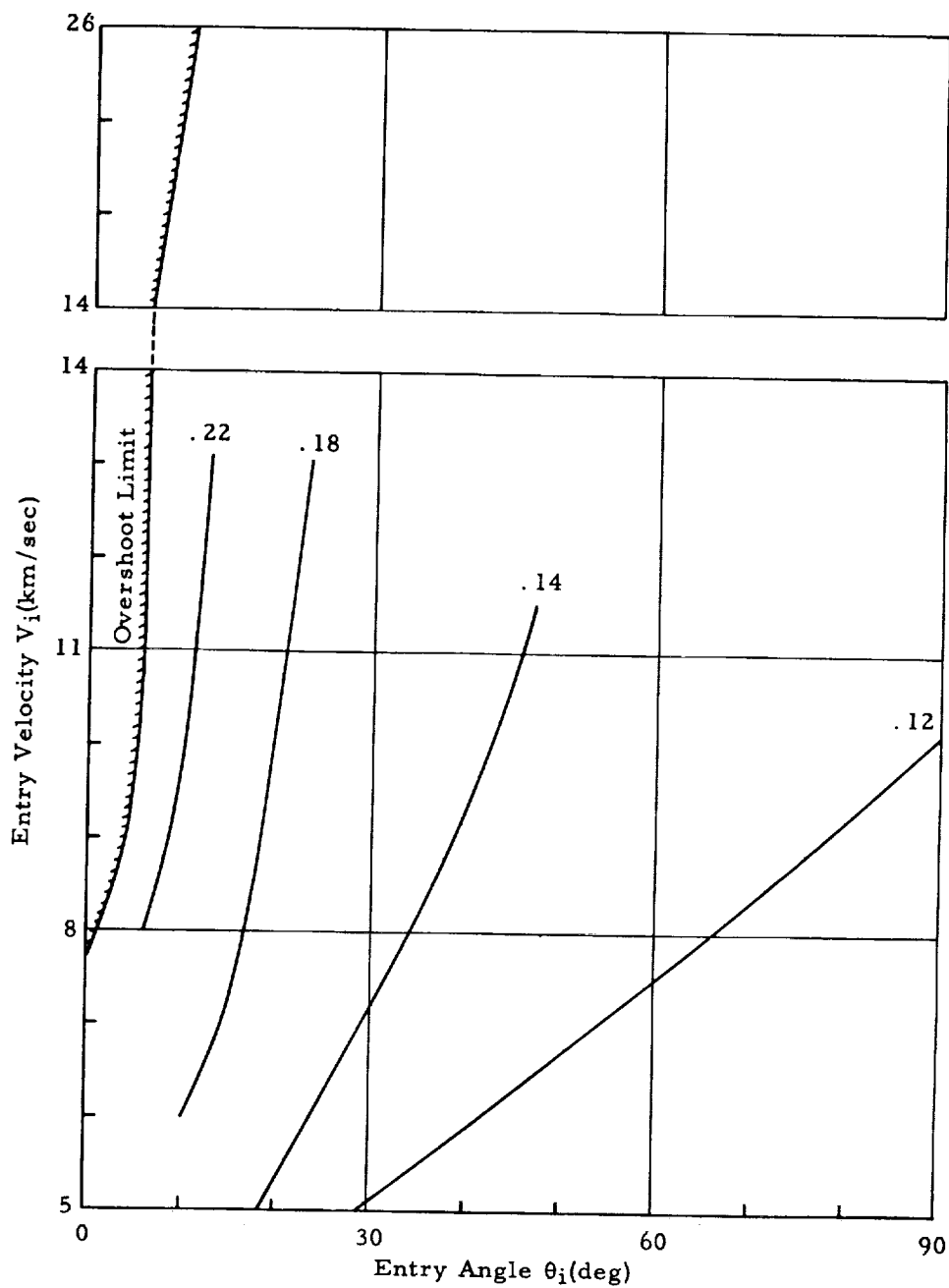


FIG. 8. RATIO OF AERODYNAMIC HEAT TRANSFER AT THE STAGNATION POINT TO KINETIC ENERGY CONVERTED INTO HEAT, $\frac{\int_0^{t_f} \bar{q}_{aero} dt}{m(0)V_i^2/2A}$

Data pertains to vapor pressure $p_{v1}(T)$ and initially hemispheric model with:
 Radius $R(0) = 1.30$ cm, i. e. $W(0) = 11.04$ grams (—)
 Radius $R(0) = 0.65$ cm, i. e. $W(0) = 1.38$ grams (---)

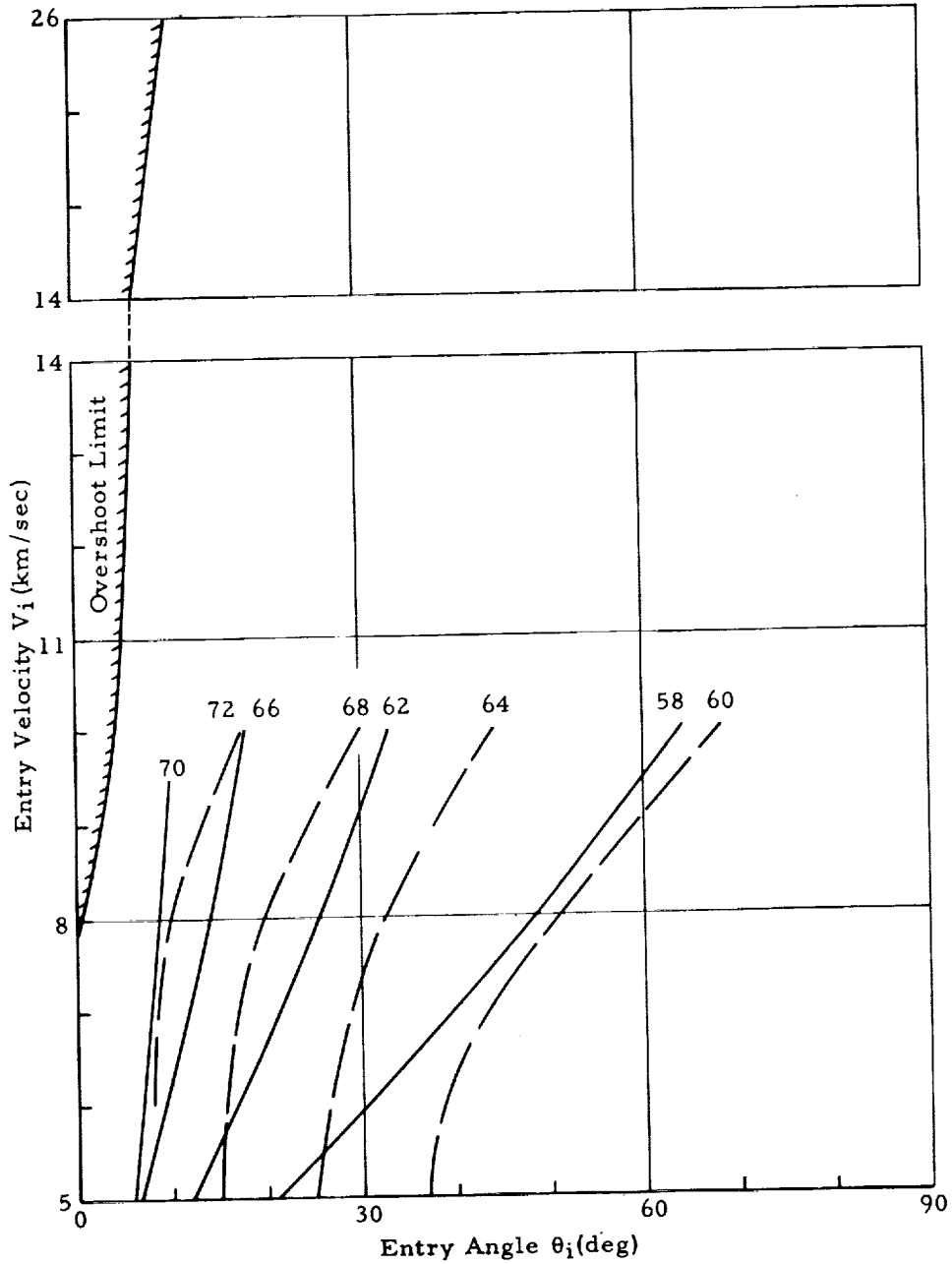


FIG. 9. ALTITUDE H (KM) OF MAXIMUM AERODYNAMIC HEAT TRANSFER AT THE STAGNATION POINT

Data pertains to vapor pressure $p_{v1}(T)$ and initially hemispheric model with:
 Radius $R(0) = 1.30$ cm, i. e. $W(0) = 11.04$ grams (———)
 Radius $R(0) = 0.65$ cm, i. e. $W(0) = 1.38$ grams (-----)

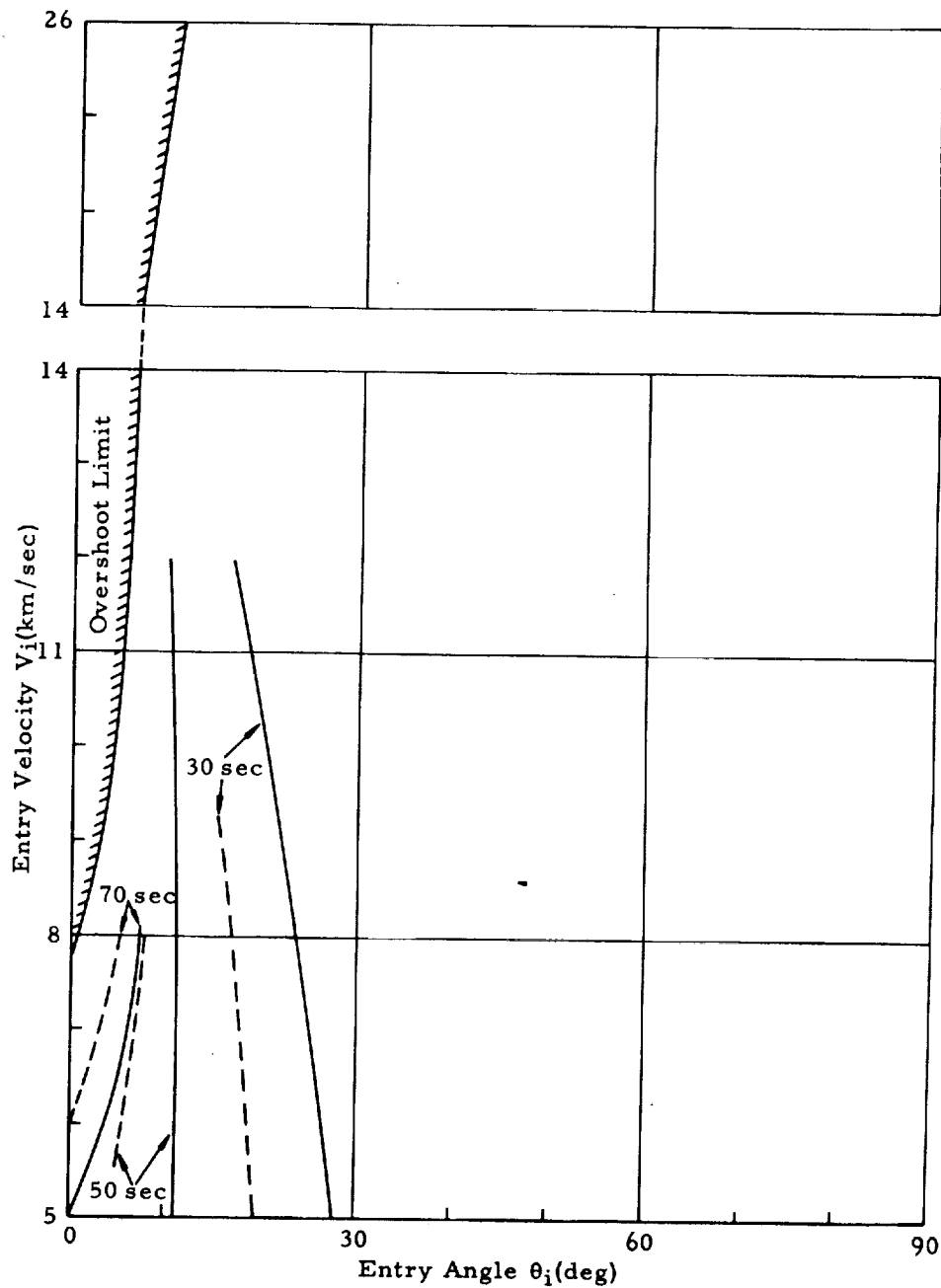


FIG. 10. DURATION OF AERODYNAMIC HEAT TRANSFER PULSE AT THE STAGNATION POINT

Data pertains to initially hemispheric model with:

- Radius $R(0) = 1.30$ cm, i.e. $W(0) = 11.04$ grams, and vapor pressure $P_{v1}(T)$ (—)
- Radius $R(0) = 0.65$ cm, i.e. $W(0) = 1.38$ grams, and vapor pressure $P_{v1}(T)$ (---)
- Radius $R(0) = 1.30$ cm, i.e. $W(0) = 11.04$ grams, and vapor pressure $P_{v2}(T)$ (-.-.-)

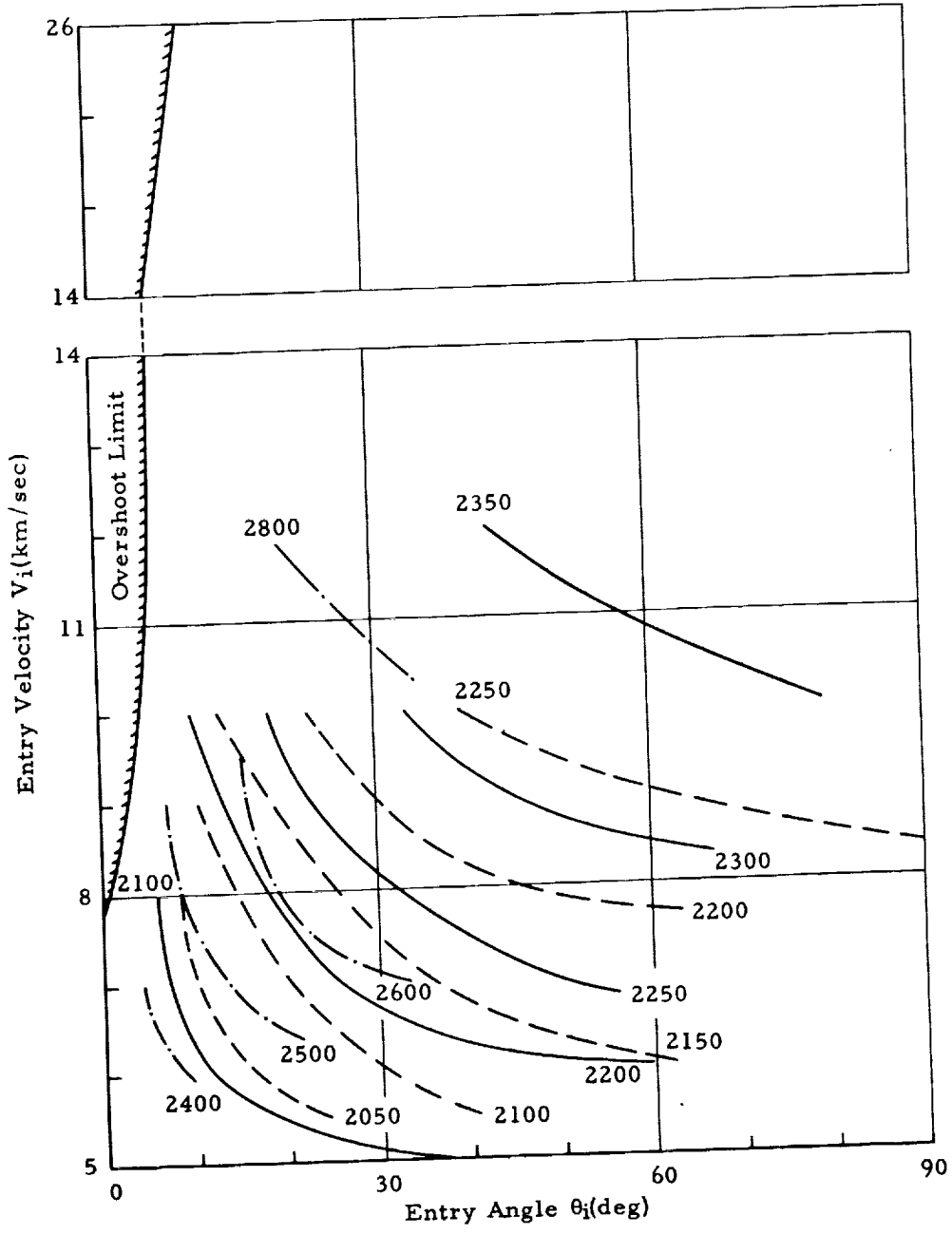


FIG. 11. MAXIMUM SURFACE TEMPERATURE $T_{s,max}$ ($^{\circ}K$) AT THE STAGNATION POINT

Data pertains to vapor pressure $p_{v1}(T)$ and initially hemispheric model with:
 Radius $R(0) = 1.30$ cm, i.e. $W(0) = 11.04$ grams (———)
 Radius $R(0) = 0.65$ cm, i.e. $W(0) = 1.38$ grams (----)

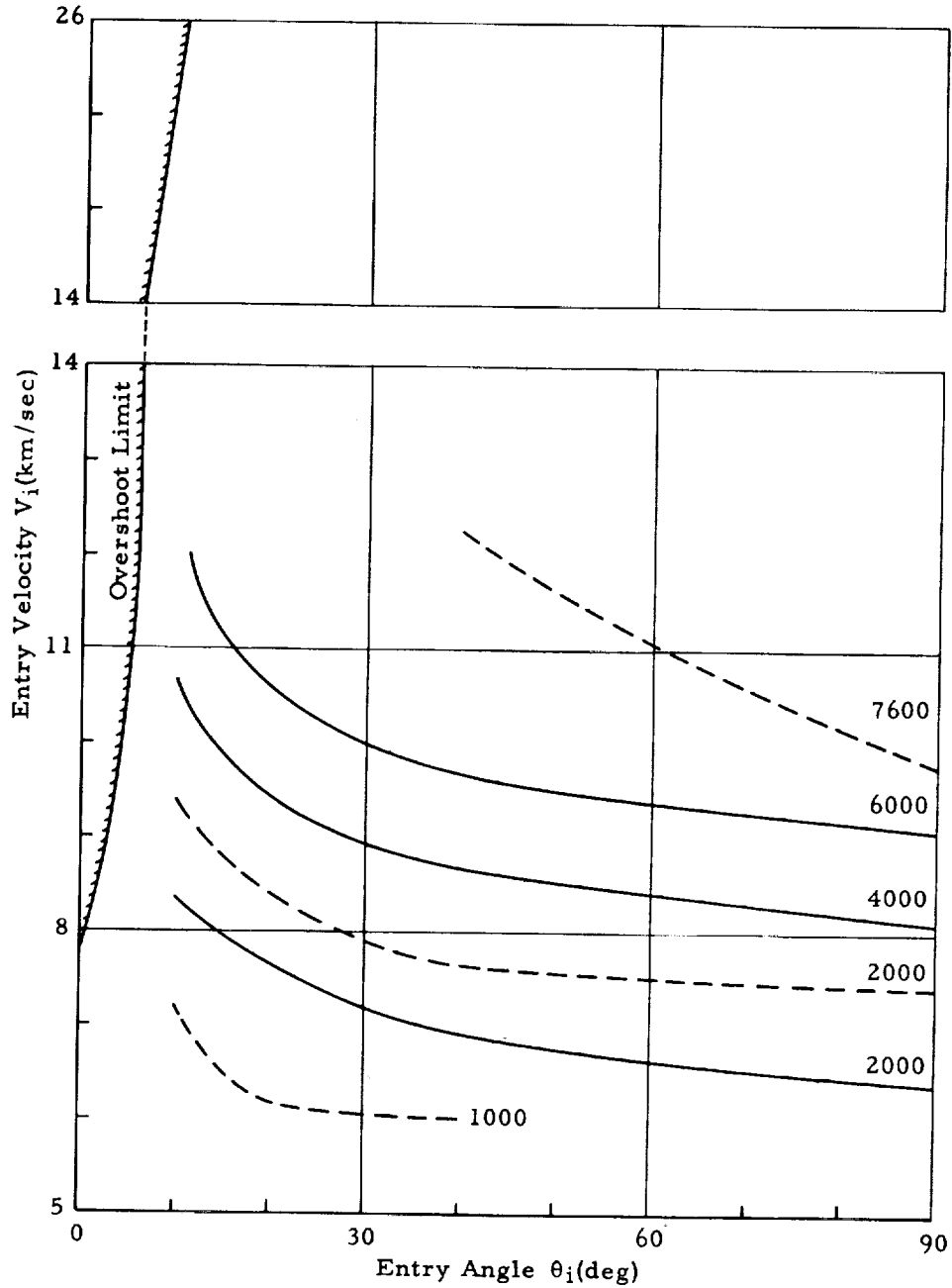


FIG. 12. MAXIMUM AERODYNAMIC HEAT TRANSFER $\bar{q}_{aero, max}$ (kcal/m²sec) AT THE STAGNATION POINT

Data pertains to initially hemispheric model with:

- Radius $R(0) = 1.30$ cm, i. e. $W(0) = 11.04$ grams, and vapor pressure $P_{V1}(T)$ (——)
- Radius $R(0) = 0.65$ cm, i. e. $W(0) = 1.38$ grams, and vapor pressure $P_{V1}(T)$ (----)
- Radius $R(0) = 1.30$ cm, i. e. $W(0) = 11.04$ grams, and vapor pressure $P_{V2}(T)$ (— · —)

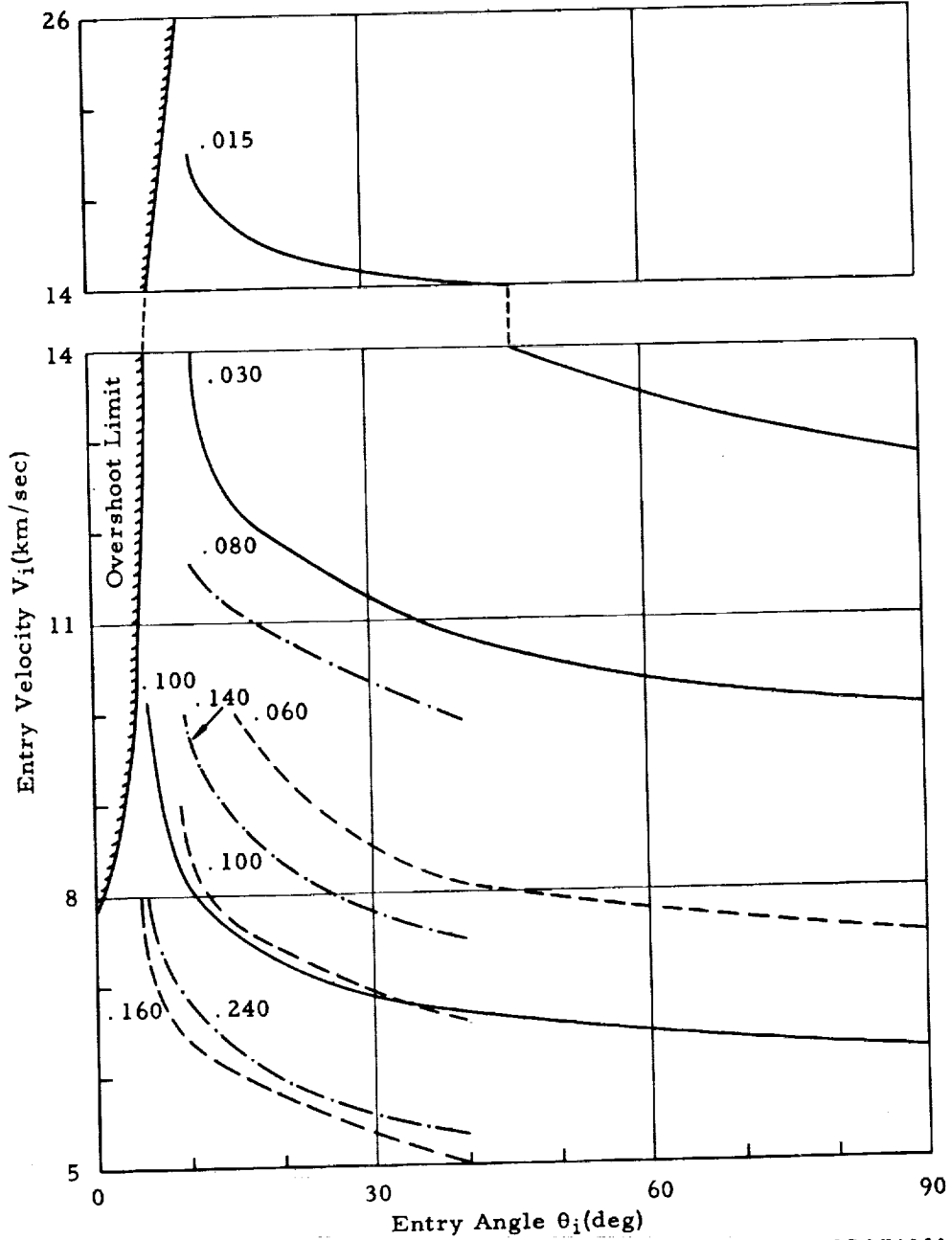


FIG. 13. RATIO OF HEAT RADIATED FROM SURFACE TO AERODYNAMIC HEATING, $\int_0^{t_f} q_{rad} dt / \int_0^{t_f} \bar{q}_{aero} dt$, AT THE STAGNATION POINT

Data pertains to initially hemispheric model with:

Radius $R(0) = 1.30$ cm, i.e. $W(0) = 11.04$ grams, and vapor pressure $p_{v1}(T)$ (—)

Radius $R(0) = 0.65$ cm, i.e. $W(0) = 1.38$ grams, and vapor pressure $p_{v1}(T)$ (- - -)

Radius $R(0) = 1.30$ cm, i.e. $W(0) = 11.04$ grams, and vapor pressure $p_{v2}(T)$ (— · —)

$q_{bl} = (\bar{q}_{aero} - q_{aero}) + \gamma h_v V_s$, where $\bar{q}_{aero} - q_{aero}$ is due to the diffusion of vapor across the boundary layer and $\gamma h_v V_s$ is the heat absorbed by the evaporation process.

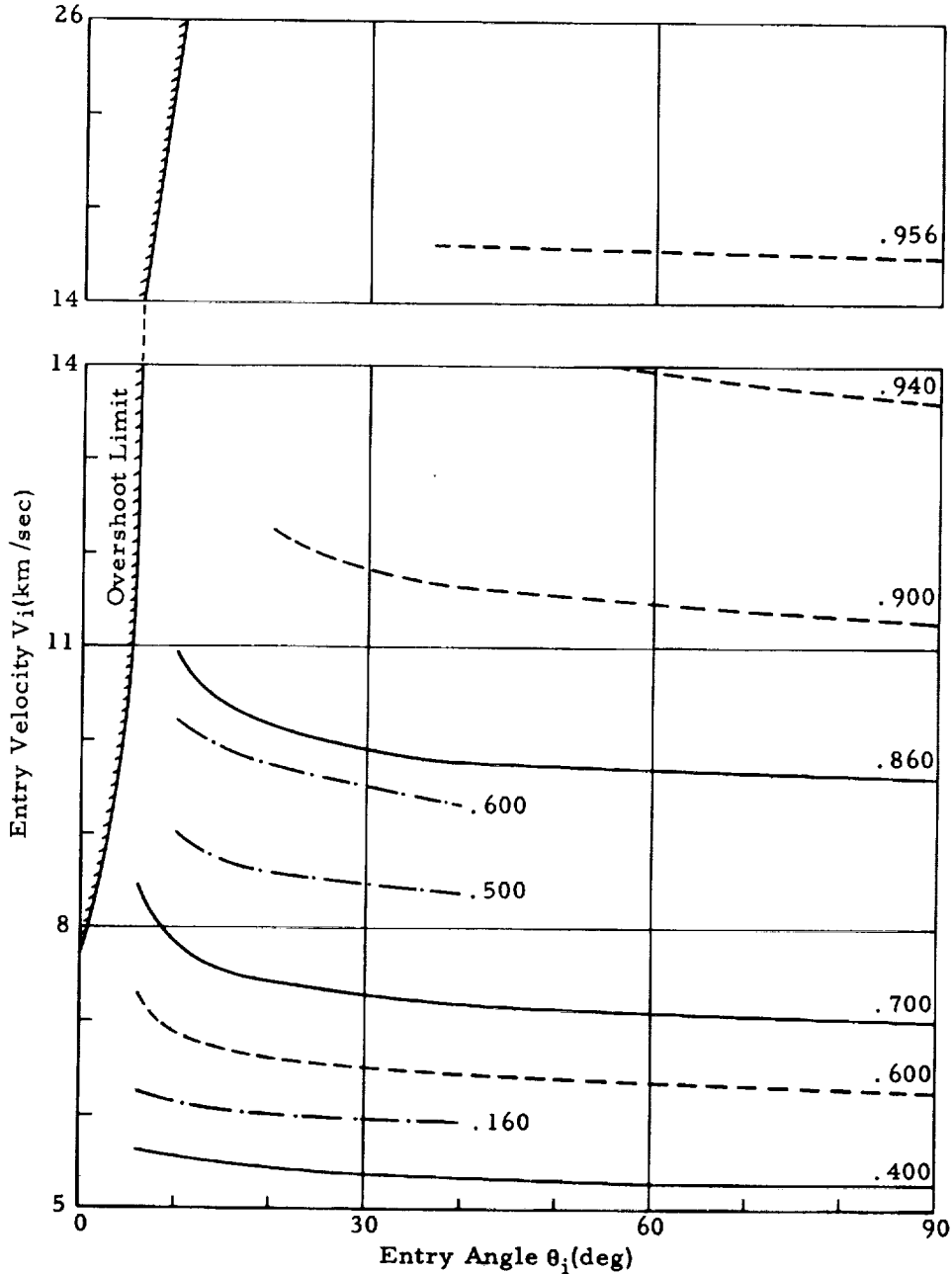


FIG. 14. RATIO OF HEAT BLOCKED BY MASS TRANSFER EFFECT TO AERODYNAMIC

HEATING, $\int_0^{t_f} q_{bl} dt / \int_0^{t_f} \bar{q}_{aero} dt$, AT THE STAGNATION POINT

Data pertains to initially hemispheric model with:

- Radius $R(0) = 1.30$ cm, i.e. $W(0) = 11.04$ grams, and vapor pressure $P_{V1}(T)$ (—)
- Radius $R(0) = 0.65$ cm, i.e. $W(0) = 1.38$ grams, and vapor pressure $P_{V1}(T)$ (---)
- Radius $R(0) = 1.30$ cm, i.e. $W(0) = 11.04$ grams, and vapor pressure $P_{V2}(T)$ (— · —)

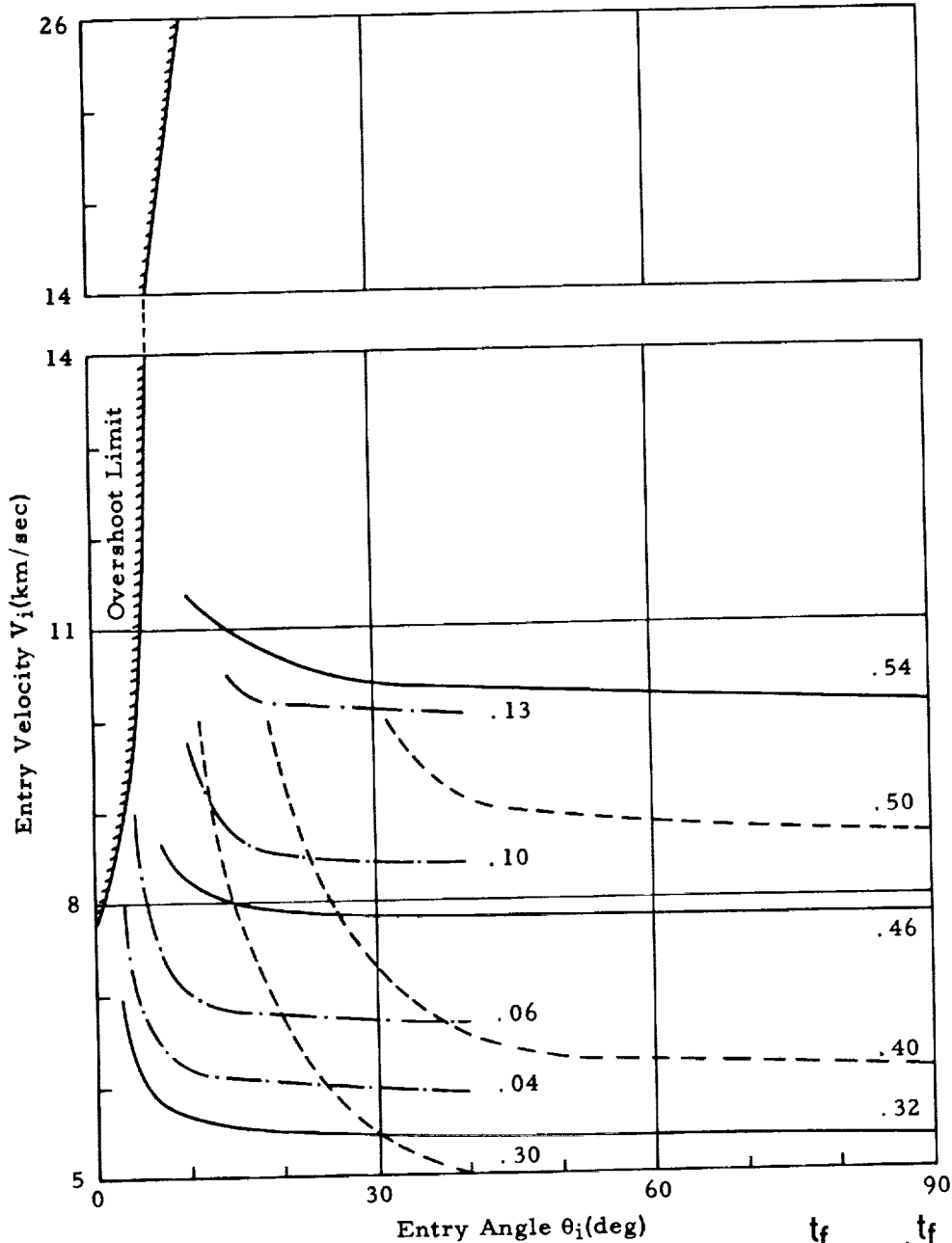


FIG. 15. RATIO OF EVAPORATION TO TOTAL ABLATION, $\int_0^{t_f} V_s dt / \int_0^{t_f} V_\infty dt$,
AT THE STAGNATION POINT

Data pertains to the particular tektite flight treated in Figures 16 - 21 and the vapor pressure $P_{v1}(T)$. The model initially is a hemisphere with radius $R(0) = 1.30$ cm, i.e. $W(0) = 11.04$ grams. Presented functions:
Flight altitude H (———)
Horizontal distance D covered in flight (----)
Flight Mach number M (— · —)

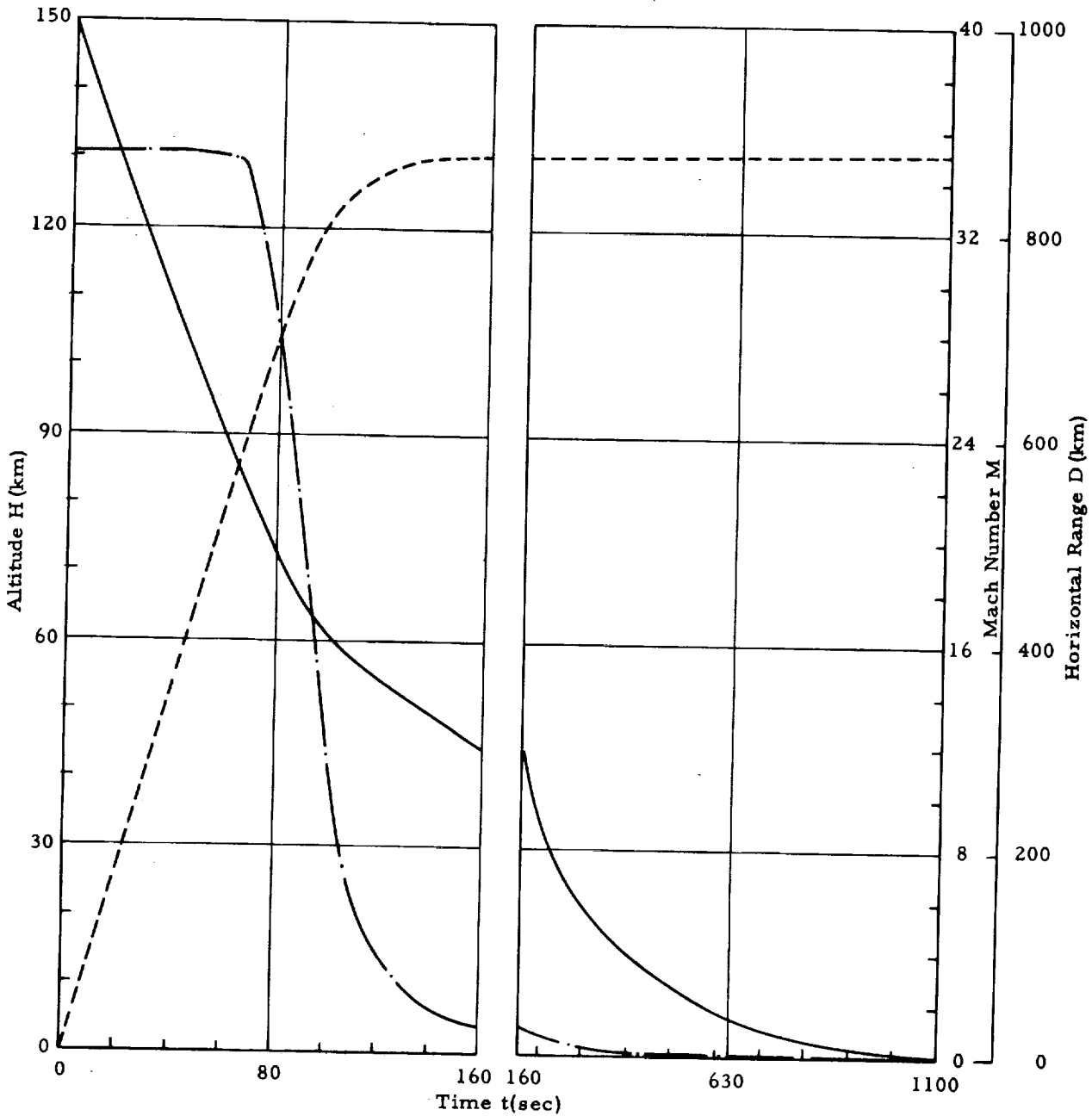


FIG. 16. FLIGHT ALTITUDE, HORIZONTAL DISTANCE, AND MACH NUMBER FOR PARTICULAR TEKTITE TRAJECTORY

Data pertains to the particular tektite flight treated in Figures 16 - 21 and the vapor pressure $p_{v1}(T)$. The model initially is a hemisphere with radius $R(0) = 1.30$ cm, i.e. $W(0) = 11.04$ grams. Presented functions:

- Flight speed V (—)
- Acceleration a (---)
- Trajectory angle θ relative to earth's horizontal (— · —)

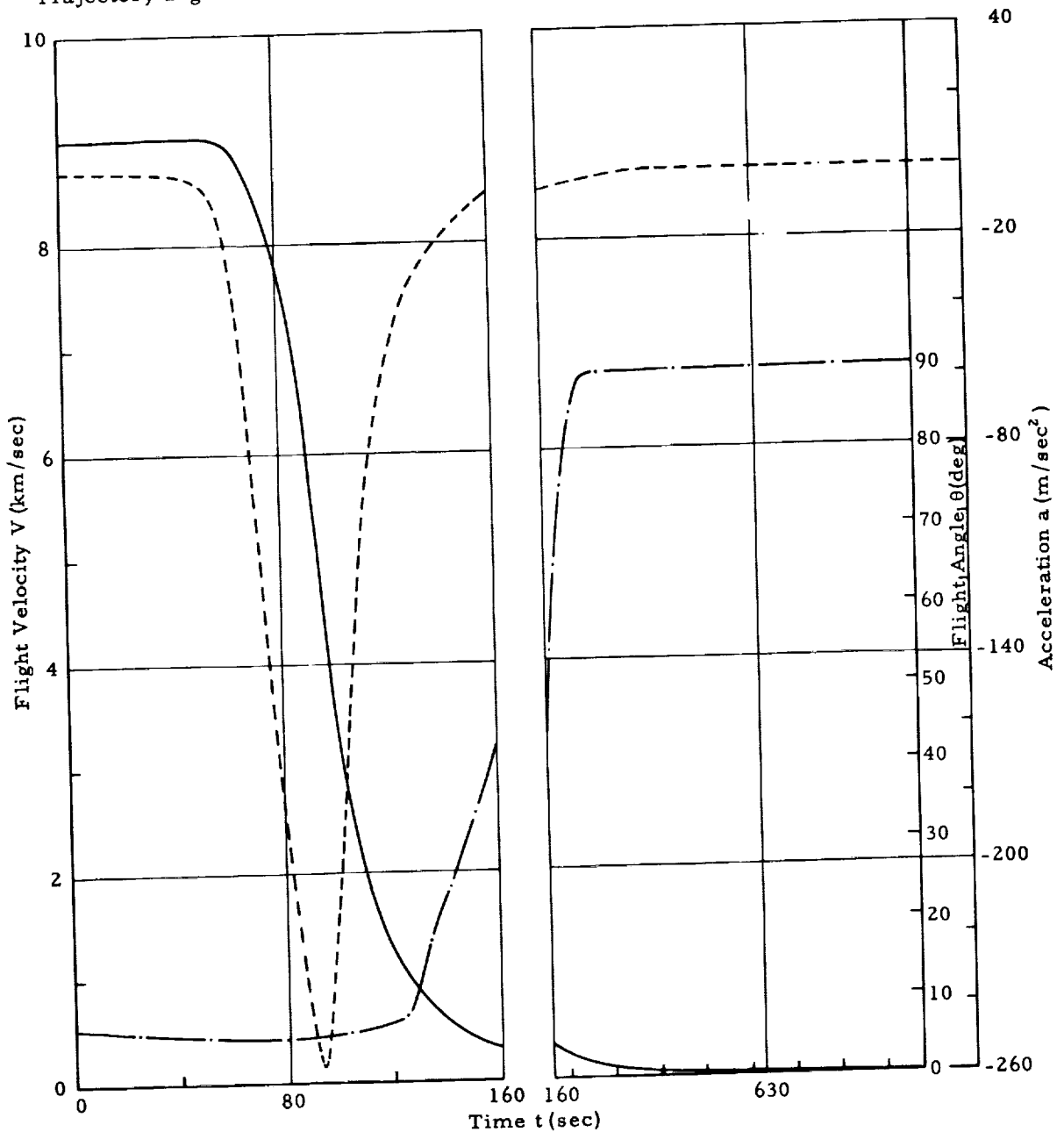


FIG. 17. FLIGHT SPEED, ACCELERATION, AND TRAJECTORY ANGLE FOR PARTICULAR TEKTITE TRAJECTORY

Data pertains to the particular tektite flight treated in Figures 16 - 21 and the vapor pressure $p_{v1}(T)$. The model initially is a hemisphere with radius $R(0) = 1.30$ cm, i. e. $W(0) = 11.04$ grams. Presented functions:

aerodynamic heat transfer rate \bar{q}_{aero} to a non-evaporating surface (—), aerodynamic heat transfer rate q_{aero} to the evaporating surface (---), heat radiated from surface, q_{rad} (-.-.-), heat blocked by mass transfer effect, q_{b1} , see legend of Fig. 14, (---), and surface temperature T_s (-.-.-), all at the stagnation point.

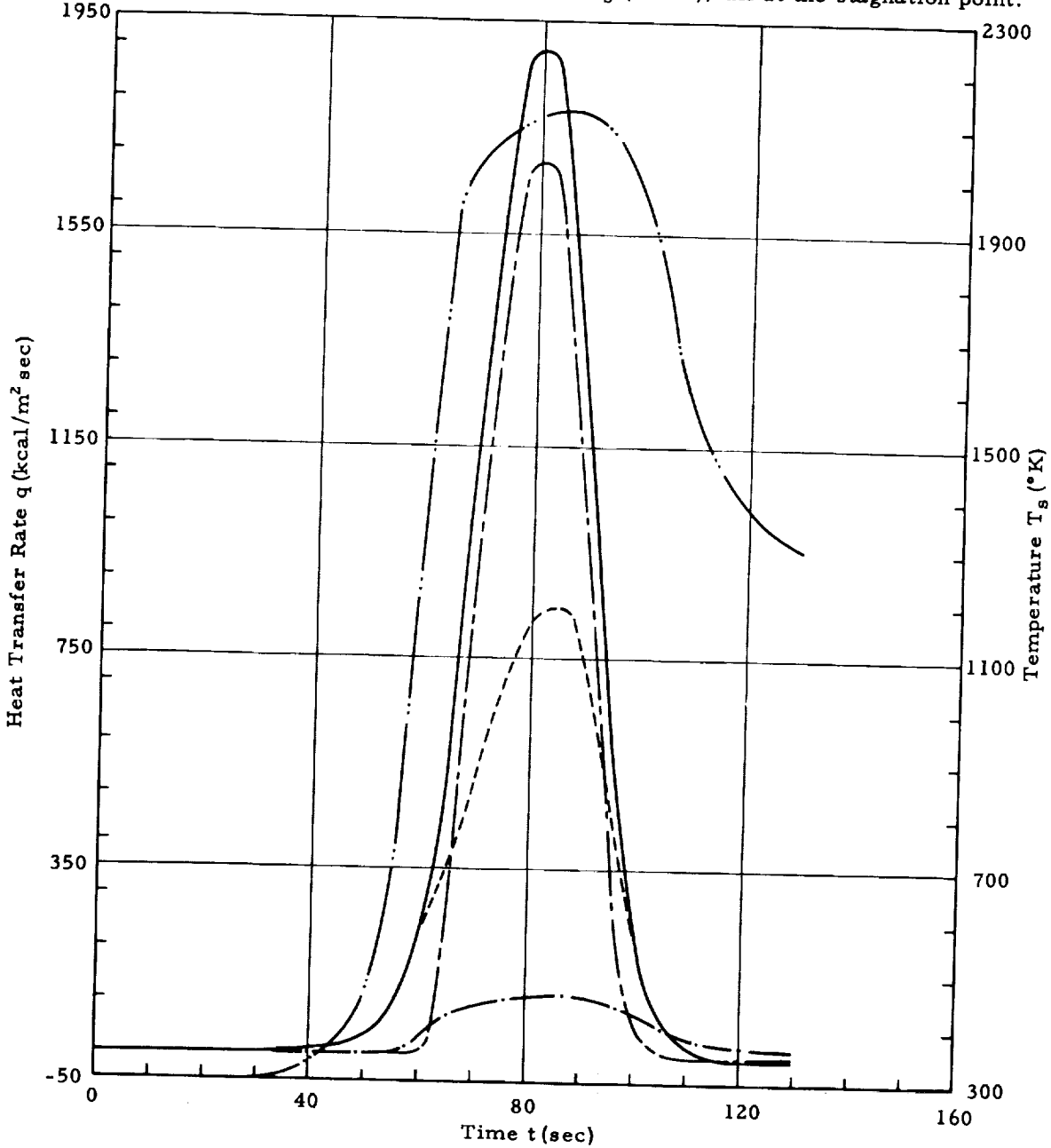


FIG. 18. HEAT FLOW RATES AND SURFACE TEMPERATURE FOR PARTICULAR TEKTITE TRAJECTORY

Data pertains to the particular tektite flight treated in Figures 16 - 21 and the vapor pressure $p_{v1}(T)$. The model initially is a hemisphere with radius $R(0) = 1.30$ cm, i.e. $W(0) = 11.04$ grams. Presented functions:

- Evaporation speed v_s of the liquid at the surface (—)
 - Thickness R^* of the model, see Fig. 4, (---)
 - Mass ratio $m(t)/m(0)$ of model (— · —)
 - Gradient du/dx of tangential velocity component of melt (— · — · —)
- All at the stagnation point.

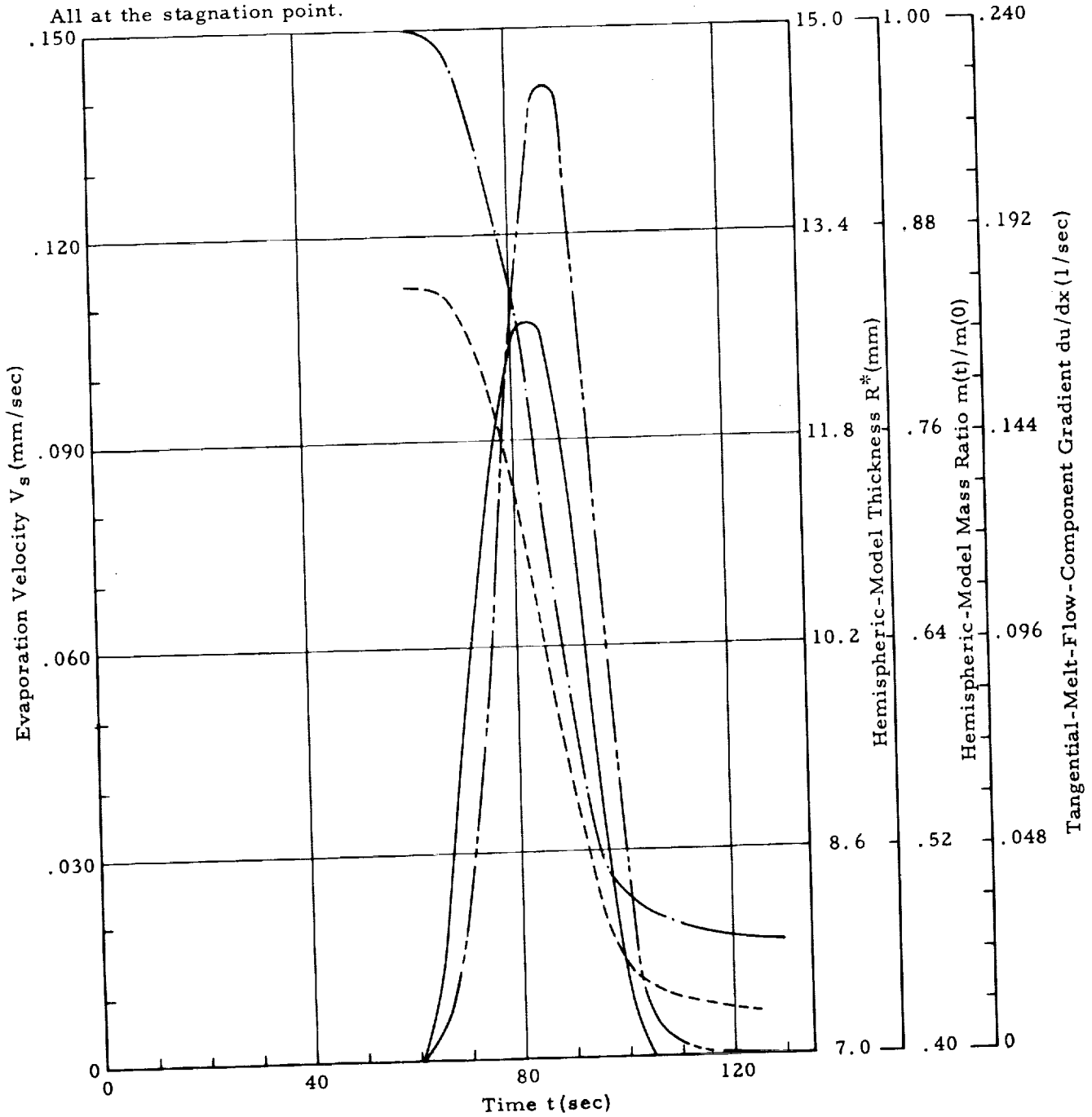


FIG. 19. ABLATION PARAMETERS FOR PARTICULAR TEKTITE TRAJECTORY

Data pertains to the particular tektite flight treated in Figures 16 - 21 and the vapor pressure $p_{v1}(T)$. The model initially is a hemisphere with radius $R(0) = 1.30$ cm, i.e. $W(0) = 11.04$ grams. The shaded lines adjacent to the instantaneous locations of the stagnation point indicate the thicknesses of the melt layer.

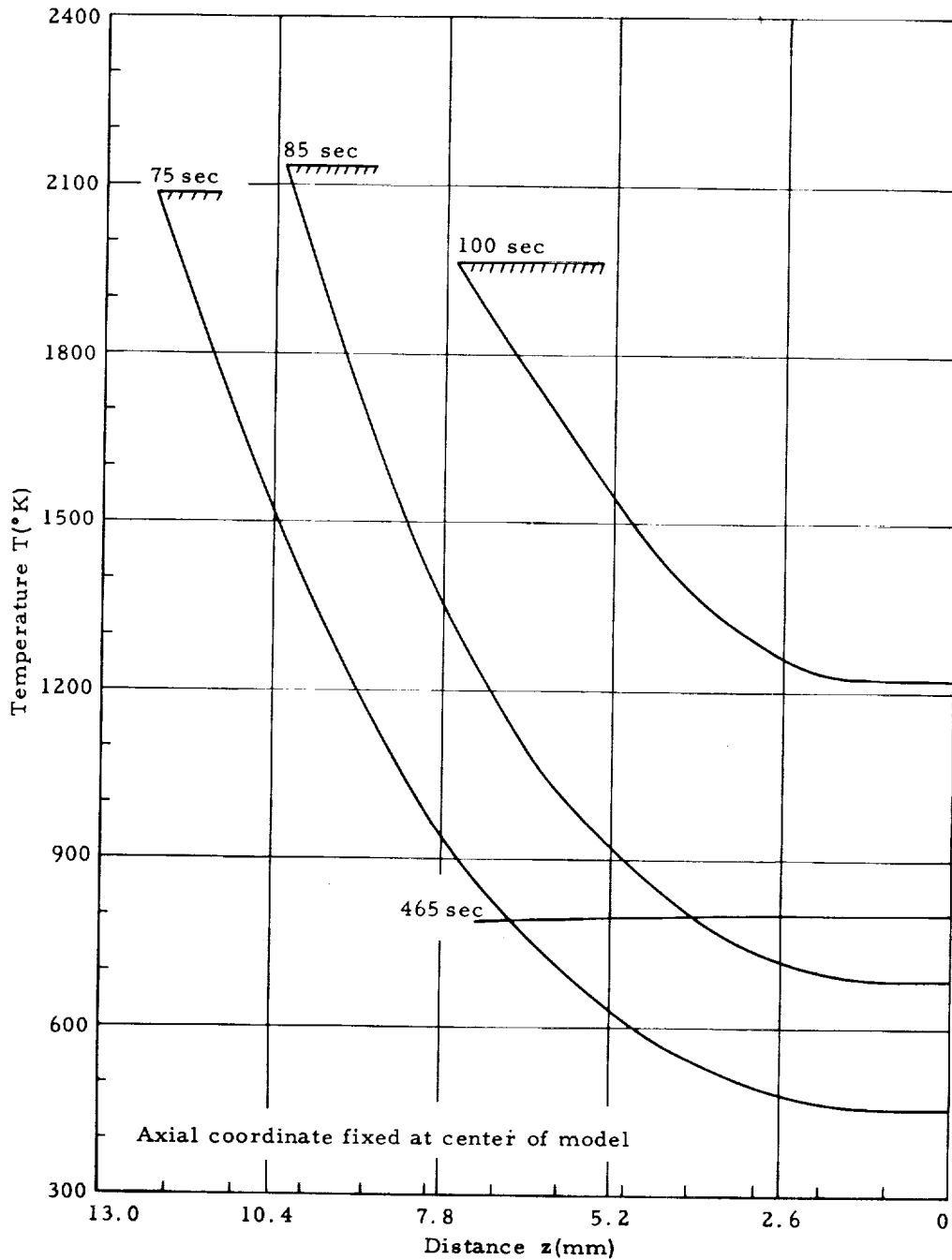


FIG. 20. TEMPERATURE DISTRIBUTION ALONG AXIS FOR PARTICULAR TEKTITE TRAJECTORY

Data pertains to initially hemispheric model with radius $R(0) = 1.30$ cm, i. e. $W(0) = 11.04$ grams, entry speed $V_i = 9$ km/sec, entry angle $\theta_i = 7^\circ$, and vapor pressure $P_{v1}(T)$.

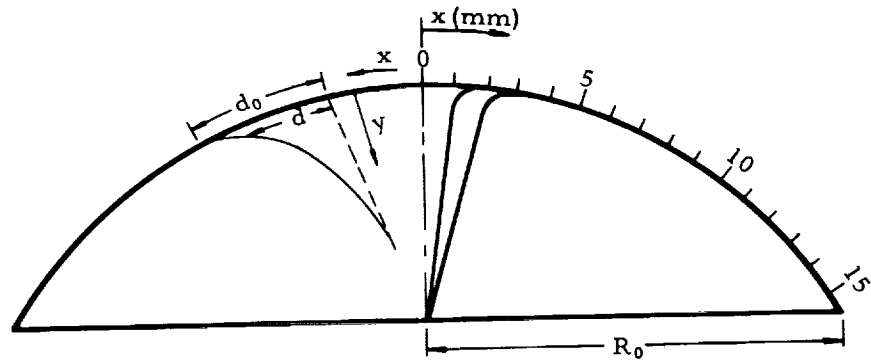


Fig. 21a. Striae After Solidification of Melt

Fig. 21c. Striae Distortion as a Function of y

Fig. 21b. Striae Distortion at the Surface as a Function of x

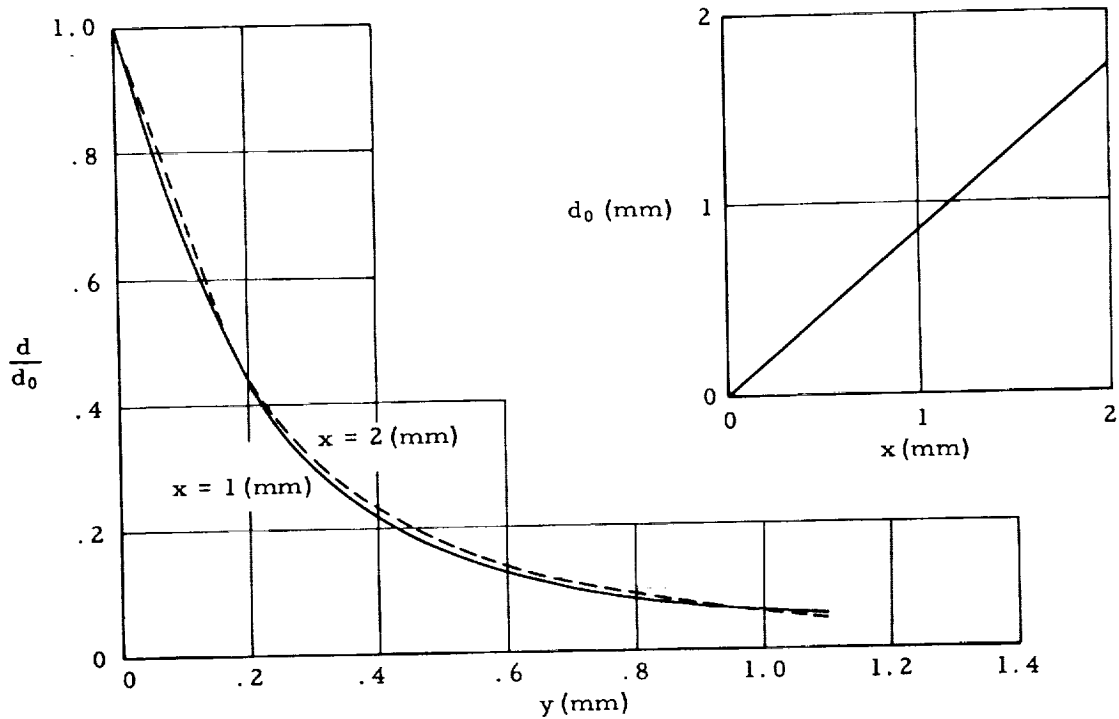


FIG. 21. STRIAE DEFORMATION FOR PARTICULAR TEKTITE TRAJECTORY, (54% MASS LOSS)

Data pertains to initially hemispheric model with radius $R(0) = 1.30$ cm, i. e. $W(0) = 11.04$ grams, entry speed $V_i = 6$ km/sec, entry angle $\theta_i = 2^\circ$, and vapor pressure $p_{v1}(T)$.

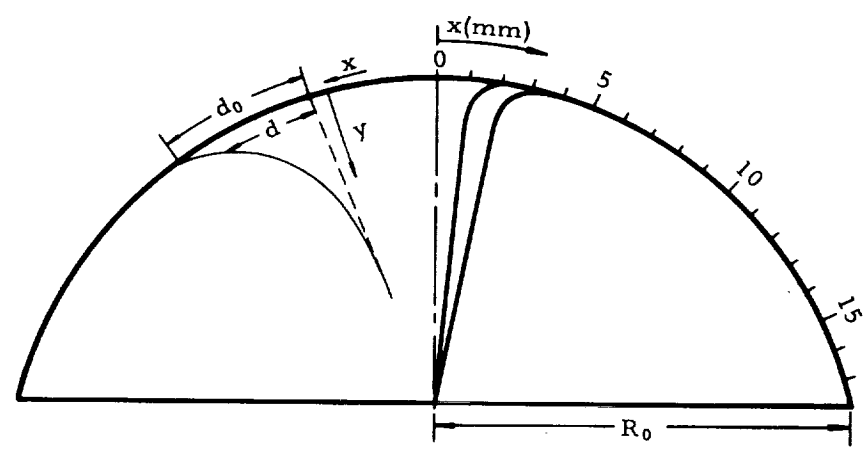


Fig. 22a. Striae After Solidification of Melt

Fig. 22c. Striae Distortion as a Function of y

Fig. 22b. Striae Distortion at the Surface as a Function of x

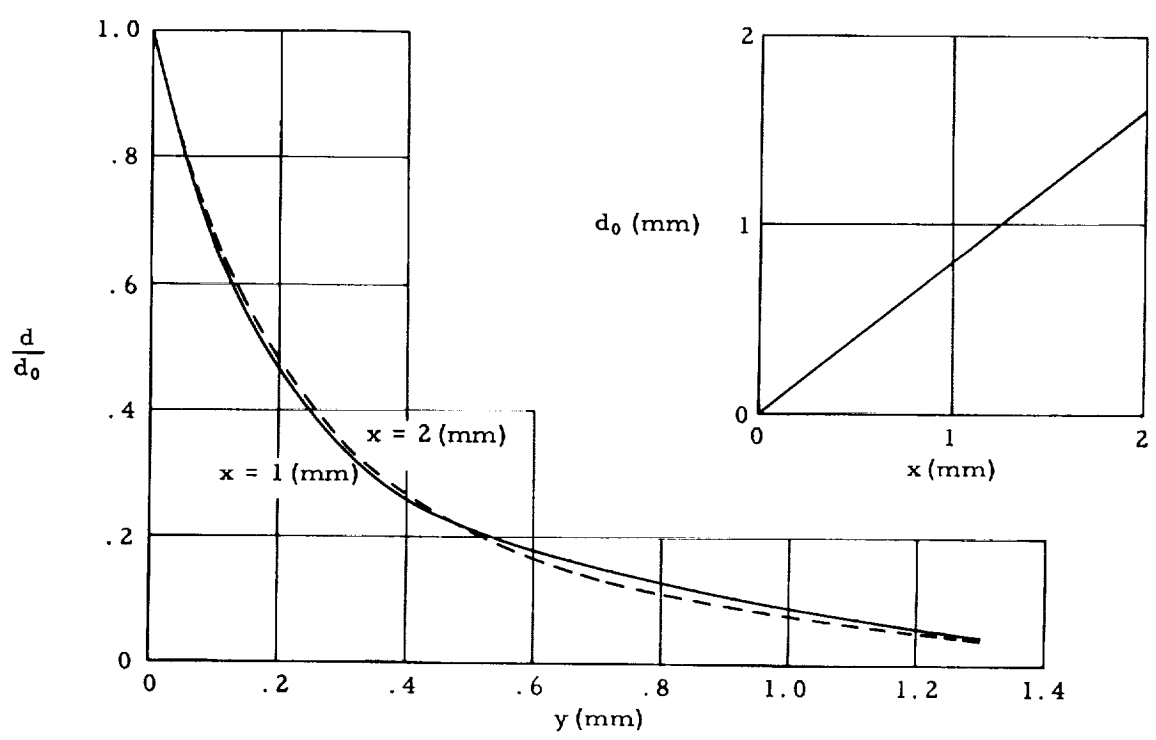
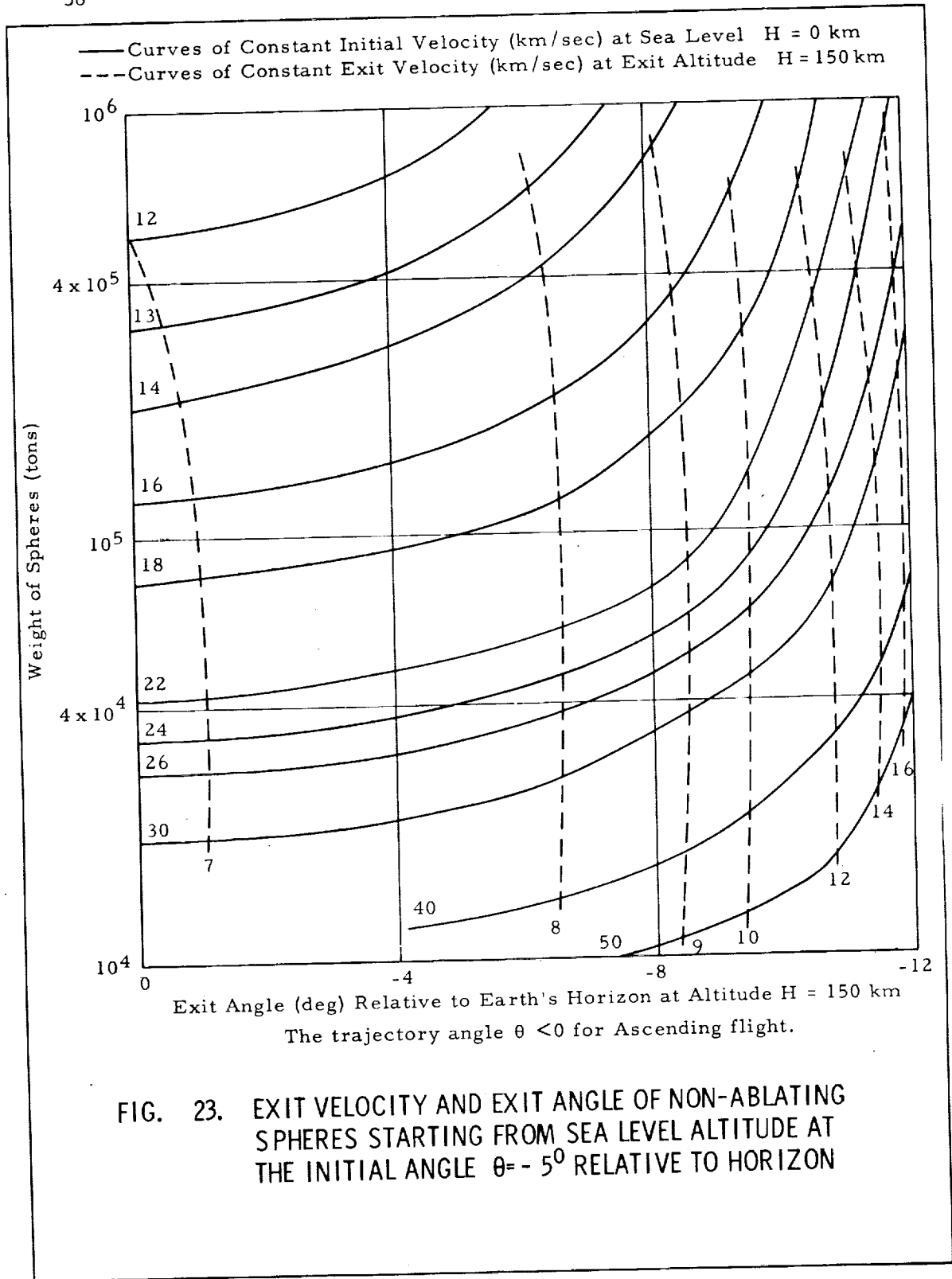
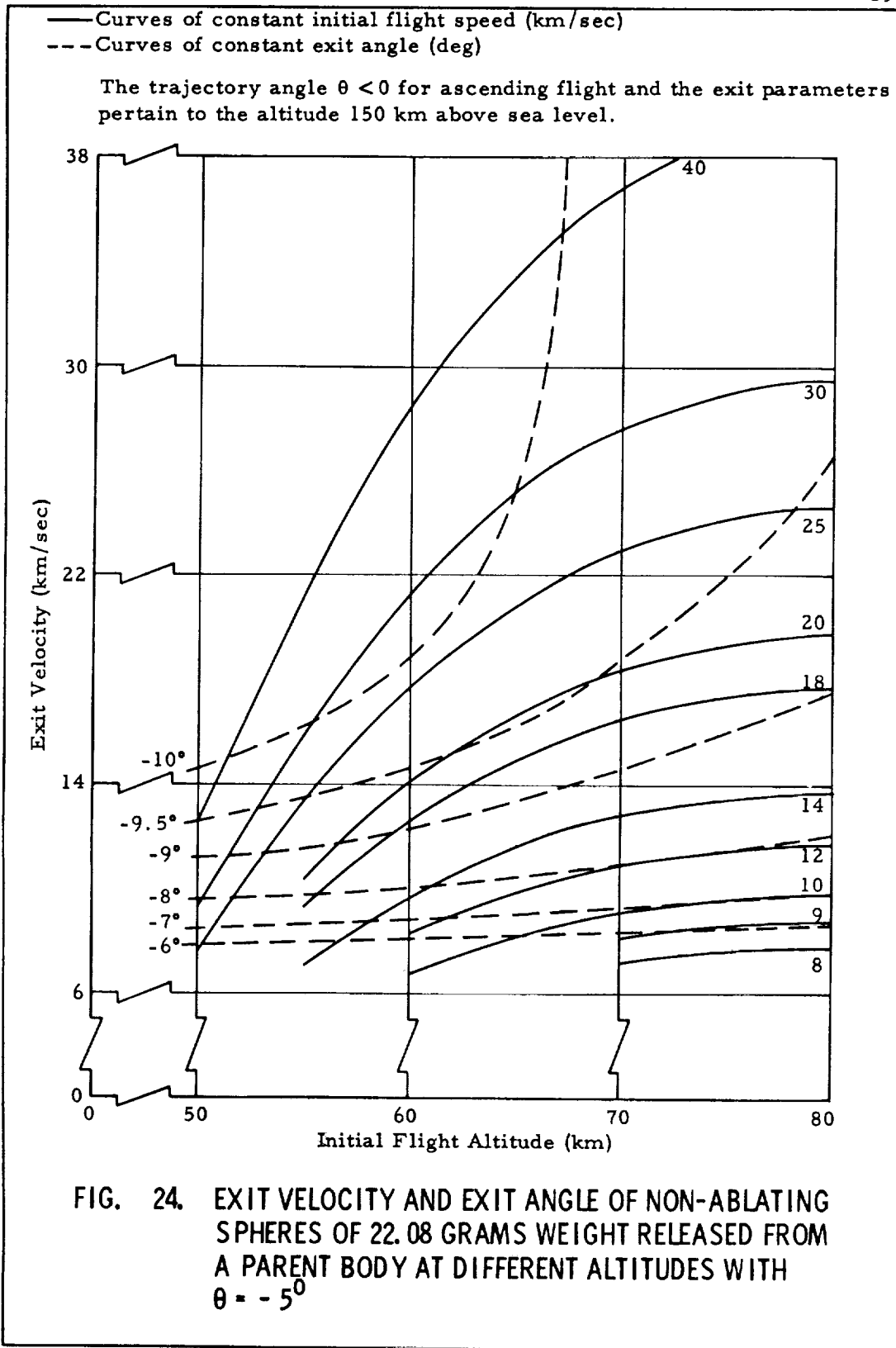


FIG. 22. STRIAE DEFORMATION FOR PARTICULAR TEKTITE TRAJECTORY, (28% MASS LOSS)





LIST OF SYMBOLS

$A = \pi R^2(0)$	cm^2	Area of maximum cross section in fig. 4
a	m/sec^2	Deceleration
α	$1/\text{m}$	Absorption coefficient for thermal radiation
c_D		Drag coefficient
c_p	$\text{kcal/kg } ^\circ\text{K}$	Specific heat at constant pressure
D	km	Horizontal range covered in flight
$g = 9.81$	m/sec^2	Gravity constant at sea level altitude
H	km	Flight altitude
h	$\text{kg/m}^2\text{sec}$	Heat transfer coefficient
h_e	kcal/kg	Enthalpy of air at outer edge of boundary layer
h_s	kcal/kg	Enthalpy of air at surface
h_v	kcal/kg	Heat of evaporation
k	$\text{kcal/m } ^\circ\text{K sec}$	Thermal conductivity
M		Flight Mach number
m	kg_m	Mass
P_e	kg/m^2	Air pressure at outer edge of boundary layer
P_{v1}	kg/m^2	Vapor pressure of kytite material
P_{v2}	kg/m^2	Vapor pressure of quartz
q_{aero}	$\text{kcal/m}^2\text{sec}$	Aerodynamic heat transfer to evaporating surface
\bar{q}_{aero}	$\text{kcal/m}^2\text{sec}$	Aerodynamic heat transfer to non-evaporating surface
q_{bl}	$\text{kcal/m}^2\text{sec}$	Heat blocked by evaporation and vapor diffusion
q_{rad}	$\text{kcal/m}^2 \text{ sec}$	Heat radiated from surface into air

LIST OF SYMBOLS (CONT'D)

R and R*	m	Defined in fig. 4
t	sec	Time
T	°K	Temperature
u	mm/sec	Velocity component of melt flow parallel to surface
v	mm/sec	Velocity component of melt flow normal to surface
v_{∞}	mm/sec	Ablation speed at stagnation point
v_s	mm/sec	Evaporation speed of melt at stagnation point
V	km/sec	Flight speed
W	gram	Weight
x	m	Coordinate parallel to surface, fig. 4
y or z	m	Coordinate normal to surface, fig. 4
γ	kg/m ³	Specific weight
ϵ		Emissivity constant
θ		Angle of flight trajectory relative to earth's horizon; $\theta > 0$ for descending flight
μ	kg sec/m ²	Viscosity
<u>Subscripts</u>		
f		final, i.e., impact time at sea level altitude
i		initial, i.e., entry time at outer edge of earth's atmosphere
max		maximum value
s		surface at stagnation point

REFERENCES AND BIBLIOGRAPHY

1. Baker, G., Tektites, Memoirs of the National Museum of Victoria, Melbourne, 1959.
2. Chao, E. C. T., I. Adler, E. D. Dwornik, and J. Littler, Metallic Spherules in Tektites from Isabela, the Philippines, Science, Jan. 1962, Vol. 135, pp. 97 - 98.
3. Viste, E. and E. Anders, Cosmic-Ray Exposure History of Tektites, The University of Chicago, The Enrico Fermi Institute for Nuclear Studies, Report EFINS 61-66, 1961.
4. Öpik, E. J., The Survival of Stray Bodies in the Solar System, Annales Academiae Scientiarum Fennicae, Series A, III Geologica-Geographica, 61, Helsinki, 1961.
5. Urey, H. C., Origin of Tektites, Nature, Vol. 179, 1957, p. 556.
6. Fenner, C., Trans. Roy. Soc. S. Australia, 62: 208, Part II, 1938.
7. Hanus, F., Rozpravy II Tridy Ces Akademie Roc, XXXVII, cis 24, 1958.
8. Hardcastle, H., New Zealand J. Science and Technol., 8:65, 1926.
9. Oswald, J., Meteorické Sklo, Práce: Nakladem České Akademie věd a Umění, 1942.
10. Chapman, D. R., H. K. Larson, and L. A. Anderson, Aerodynamic Evidence Pertaining to the Entry of Tektites into the Earth's Atmosphere, NASA Technical Report R - 134, Washington, January 1962.
11. Adams, E. W., Analysis of Quartz and Teflon Shields for a Particular Re-Entry Mission, Proceedings of the 1961 Heat Transfer and Fluid Mechanics Institute, Stafford University Press, 1961, pp. 222 - 236.
12. Bethe, H. A. and M. C. Adams, A Theory for the Ablation of Glassy Materials, Journal of the Aerospace Sciences, Vol. 26, June 1959, p. 321.
13. Chapman, D. R., Recent Re-Entry Research and the Cosmic Origin of Tektites, Nature, Vol. 188, Oct. 1960, pp 353 - 355.
14. Adams, E. W. and R. M. Huffaker, Application of Ablation Analysis to Stony Meteorites and the Tektite Problem, Nature, Vol. 193, March 1962, pp. 1249 - 1251.

REFERENCES AND BIBLIOGRAPHY (Cont'd)

15. Adams, E. W., A Comparison of Transient and Quasi-Steady Performance of Melting-Type Re-Entry Shields, *Journal of the Aerospace Sciences*, Vol. 27, Nov. 1960, pp. 791-792.
16. Grant, K., *Proceedings Roy. Soc. Victoria*, Vol. 21 (2), 1909, pp. 444 - 448.
17. Volarovich, M. P. and A. A. Leontieva, C. R. (Doklady) *Acad. Sci. U.S.S.R.*, Vol. 22, 1939.
18. Schick, H. L., Analysis of some of the Physical and Chemical Properties of Silica (SiO_2) of Importance in Ablation Behavior, AVCO Report RAD-TR-2-59-6.
19. O'Keefe, J. A., The Origin of Tektites, NASA Tech. Note D-490, Washington, Nov. 1960.
20. O'Keefe, J. A. and B. E. Shute, Tektites and Natural Satellites of The Earth, *Aerospace Engineering*, July 1960, p. 26.
21. Adams, M. C., W. E. Powers, and S. Georgiev, An Experimental and Theoretical Study of Quartz Ablation at the Stagnation Point, AVCO Research Report 57, 1959.
22. Eckert, E. R. G. and R. M. Drake, Jr., *Heat and Mass Transfer*, McGraw-Hill Book Co., New York, London, Toronto, 1959.
23. Öpik, E. J., *Physics of Meteor Flight in the Atmosphere*, Interscience Publishers, Inc., New York, 1958.
24. Wing, L. D., Radiative Heat Transfer to Hemispheric Noses, *Journal of the American Rocket Society*, Dec. 1961, pp. 90 - 92.

1
2
3
4

1
2
3
4
5
6
7
8
9
10
11
12
13
14
15
16
17
18
19
20
21
22
23
24
25
26
27
28
29
30
31
32
33
34
35
36
37
38
39
40
41
42
43
44
45
46
47
48
49
50
51
52
53
54
55
56
57
58
59
60
61
62
63
64
65
66
67
68
69
70
71
72
73
74
75
76
77
78
79
80
81
82
83
84
85
86
87
88
89
90
91
92
93
94
95
96
97
98
99
100